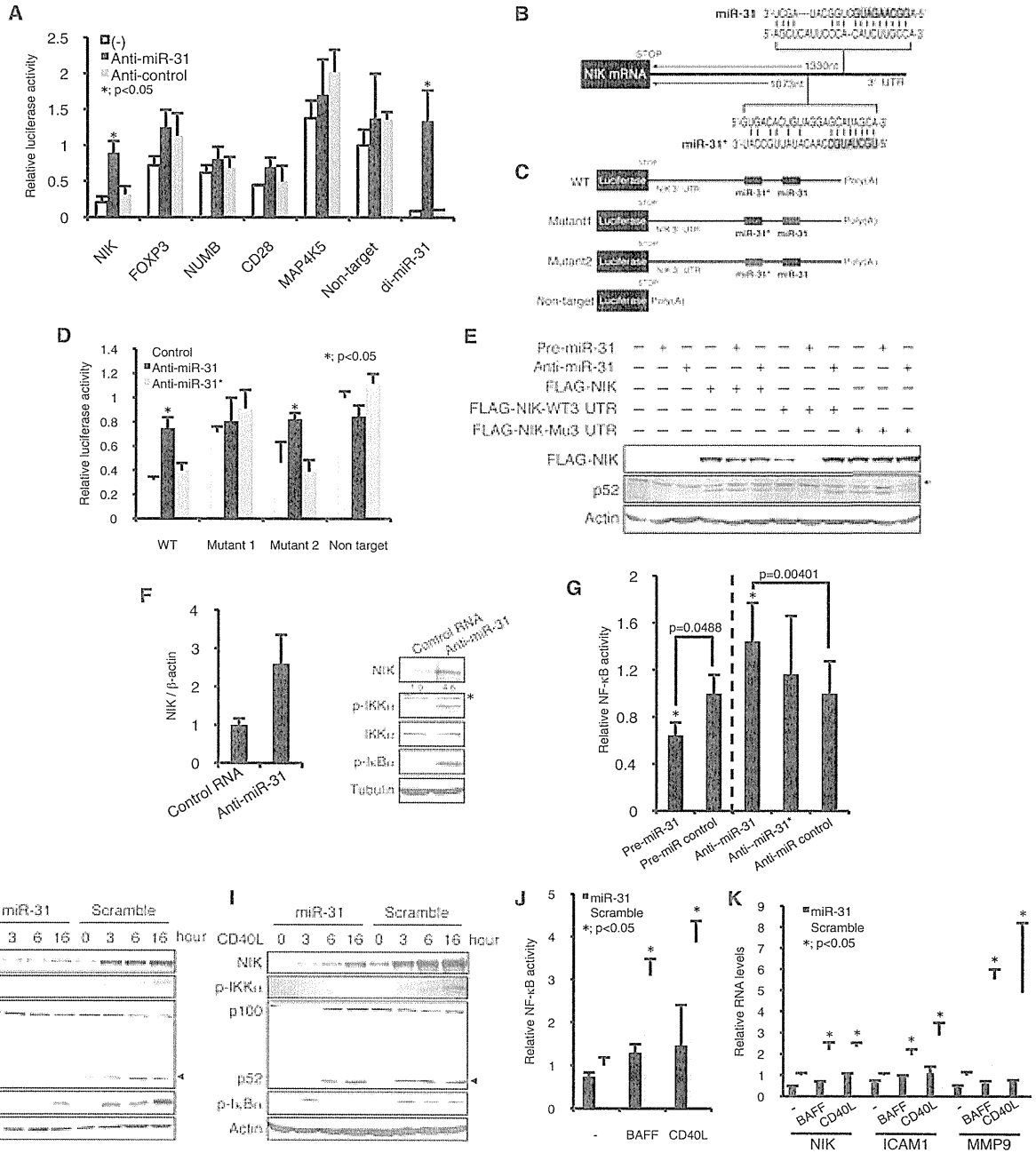

Figure 2. miR-31 Is a Negative Regulator of NF-κB Pathway by Inhibiting NIK Expression

(A) Reporter-based miR-31's target gene screening. A series of 3′ UTR-luciferase reporters was transfected in HeLa cells together with or without miR-31 specific inhibitory RNA (Anti-miR-31) or control RNA (Anti-control). Relative values of Dual-luciferase assay are presented. "Non-target" represents reporter without any 3′ UTR. "di-miR-31" reporter contains two perfect match sequences. The data are presented as mean ± SD of three independent experiments.

(B) Schematic of miR-31 target sites in the *NIK* 3′ UTR.

(C) Mutation-induced reporters. Red box stands for mutated target region (see Figure S1C).

(D) miR-31 negatively regulates *NIK* 3′ UTR analyzed by reporter assay (n = 4, mean ± SD). Luciferase activities of reporter series were tested in a presence or absence of miR-31 inhibitor.

(E) FLAG-tagged NIK protein is negatively regulated through its 3′ UTR and miR-31 binding. Plasmid vectors and miR-31 precursor or miR-31 inhibitor are cotransfected in 293T cells. Western blots showed levels of NIK and endogenous p52. Asterisk indicates nonspecific bands.

(F) NIK mRNA (left) and protein (right) levels in HeLa cells measured by quantitative RT-PCR (n = 3, mean ± SD) and western blotting, respectively. Treatment of miR-31 inhibitor resulted in NIK accumulation. Result of densitometry is shown in the bottom panel. Asterisk indicates nonspecific bands.

(G) Cellular NF-κB activity in HeLa cells (n = 5, mean ± SD) in a presence or absence of miR-31 precursor or inhibitor.

NF-κB activity (Figure 2G). Furthermore, enforced miR-31 expression in B cells attenuated both BAFF and CD40L-mediated NIK accumulation and the subsequent NF-κB signaling (Figures 2H–2K). Consistent with previous reports (Ramakrishnan et al., 2004; Zarnegar et al., 2008b), we also found decreased levels of IκBα phosphorylation. On the other hand, TNF-α-triggered canonical NF-κB activation was not affected by miR-31 in Jurkat cells (Figures S1H–S1K). These results collectively show that miR-31 inhibits the basal and receptor-initiated activities of noncanonical NF-κB pathway. With genetic evidence and an experimental approach, we further demonstrated that the function of miR-31 is well conserved among several classes of species (Figures S1L–S1O). Taking together all these results, miR-31, which is almost completely absent in primary ATL cells, appears to play a critical role in negative regulation of the NF-κB pathway by manipulating the expression of NIK.

miR-31 Suppresses ATL Cell Growth and Promotes Apoptosis by Inhibiting NF-κB

Although it was documented that abnormal NIK accumulation in ATL cells acts as a constitutive activator of the NF-κB pathway, the mechanism underlying overproduction of NIK remains to be elucidated. The results described in the previous section indicated that the amount of miR-31 is linked to the level of NIK, and we therefore speculated that downregulation of miR-31 expression is at least partially responsible for the constitutive activation of NF-κB in ATL cells. Quantitative RT-PCR revealed that *NIK* mRNA levels were negatively correlated with miR-31 levels in primary ATL cell samples (Figure 3A). To investigate the functional roles of NIK and miR-31, we established TL-Om1 cells stably expressing the miR-31 or NIK specific shRNA (shNIK) by retroviral vectors. RT-PCR and western blots showed that expression of miR-31 or shNIK reduced NIK at mRNA and protein levels as well as the levels of phospho-IKKα/β, p52, and IκBα (Figures 3B and 3C). Decreased levels of nuclear RelA and RelB are considered to represent repressed activities of the canonical and noncanonical NF-κB pathways, respectively (Figure 3D). EMSA and NF-κB reporter assays also revealed the repressive function of miR-31 and shNIK on the NF-κB activity (Figures 3E and 3F; Figures S2A, S2B, S5B, and S5C). Re-expression of NIK led to NF-κB activation that was inhibited by miR-31, suggesting a reciprocal relationship between the level of miR-31 and that of NIK.

We and others previously showed that constitutive NF-κB activation is a strong driver of ATL proliferation and prosurvival properties. Here, we examined the effects of miR-31 loss on ATL cell growth. We found that TL-Om1 cells expressing miR-31 or shNIK showed a significant attenuation of cell proliferation compared with control cells. In addition, serum starvation experiments showed greater sensitivity to induced cell death in NIK-repressed cells (Figure 3G). miR-31 expression showed the same phenotypic results in other ATL-derived cell lines (Figures S2C, S2D, and S5E). Jurkat cells do not have significant basal activity of NF-κB, and showed no significant difference in cell growth with or without induced expression of miR-31 (Figure S2E).

Next, we hypothesized that miR-31-mediated NF-κB modulation may affect cellular apoptosis, because numerous studies have demonstrated that NF-κB activation is a strong antiapoptotic factor in ATL and other cancer cells. We found that repression of NIK by miR-31 or shNIK resulted in downregulation of a subset of genes involved in resistance to apoptosis such as BCL-XL, XIAP, and FLIP (Figure 3H), suggesting that miR-31 has a role in proapoptosis through inhibition of NF-κB activity. To assess the biological function of miR-31 in apoptosis signals, we utilized a lentivirus gene transfer system for cell lines and freshly isolated tumor cells. The lentivirus vector is competent to infect nondividing cells and the infected cells can be monitored by the fluorescence of Venus. We found that lentivirus-mediated miR-31 expression promoted basal and Fas-directed apoptosis in TL-Om1 cells (Figure 3I). Venus-negative population showed no significant changes, demonstrating the specificity of miR-31 activity. To confirm the relationship among miR-31, NIK, and NF-κB signaling, we also prepared another retroviral vector encoding NIK without its 3′ UTR sequence. As results, re-expression of NIK reversed the miR-31-mediated apoptosis. In addition, miR-31 expression led to caspase 3 activation (Figure 3J). Collectively, these findings indicate that miR-31 mediates apoptosis through repression of NIK in ATL cell lines.

Tumor cells from ATL patients primarily represent the malignant characteristics. In fact, miR-31 loss is found from patient samples (Figures 1 and 3A). To demonstrate the responsibility of miR-31 for tumor cell survival, we tested whether lentivirus-mediated miR-31 expression has a killing effect against tumor cells. After establishment of lentivirus infection, the apoptotic cells were determined by flow cytometry. The results revealed that expression of miR-31 facilitated tumor cell death. Since NIK repression by shRNA lentivirus also showed a strong killing effect, NIK and NF-κB activity are suggested as crucial players for survival in ATL tumor cells (Figure 3K). Strong toxicities were not observed in normal resting lymphocytes that express low levels of NIK. Taken together, these lines of experimental evidence, including data from cell lines and primary ATL cells, definitively support two notions that (1) miR-31 acts as a tumor suppressor in T cells, and (2) NIK-regulated NF-κB has pivotal importance in cancer cell survival.

Loss of miR-31 Occurs in T Cells with Genetic and Epigenetic Abnormalities

The results described above together with previous publications indicate that regulation of miR-31 expression has profound impacts on multiple functions in human tumors as well as in normal cells. However, little is known about the regulatory mechanism of miR-31 expression. The human gene that encodes miR-31, *hsa-miR-31*, is located at 9p21.3, which is

(H–K) miR-31 attenuates signal-dependent NF-κB activation in B cells. (H and I) BJAB cells expressing miR-31 or control RNA were treated with BAFF (0.2 μg/ml) or CD40L (0.5 μg/ml) for indicated time periods. The protein levels of NIK, phospho-IKKα/β, p100/p52 (arrowheads indicate active p52), and phospho-IκBα were shown. Actin was detected as control. (J) NF-κB activity (n = 5, mean ± SD) evaluated by NF-κB-luciferase reporter assay at 24 hr after cytokine treatments. (K) NF-κB-dependent gene expressions were inhibited by miR-31 (n = 3, mean ± SD). See also Table S2 and Figure S1.

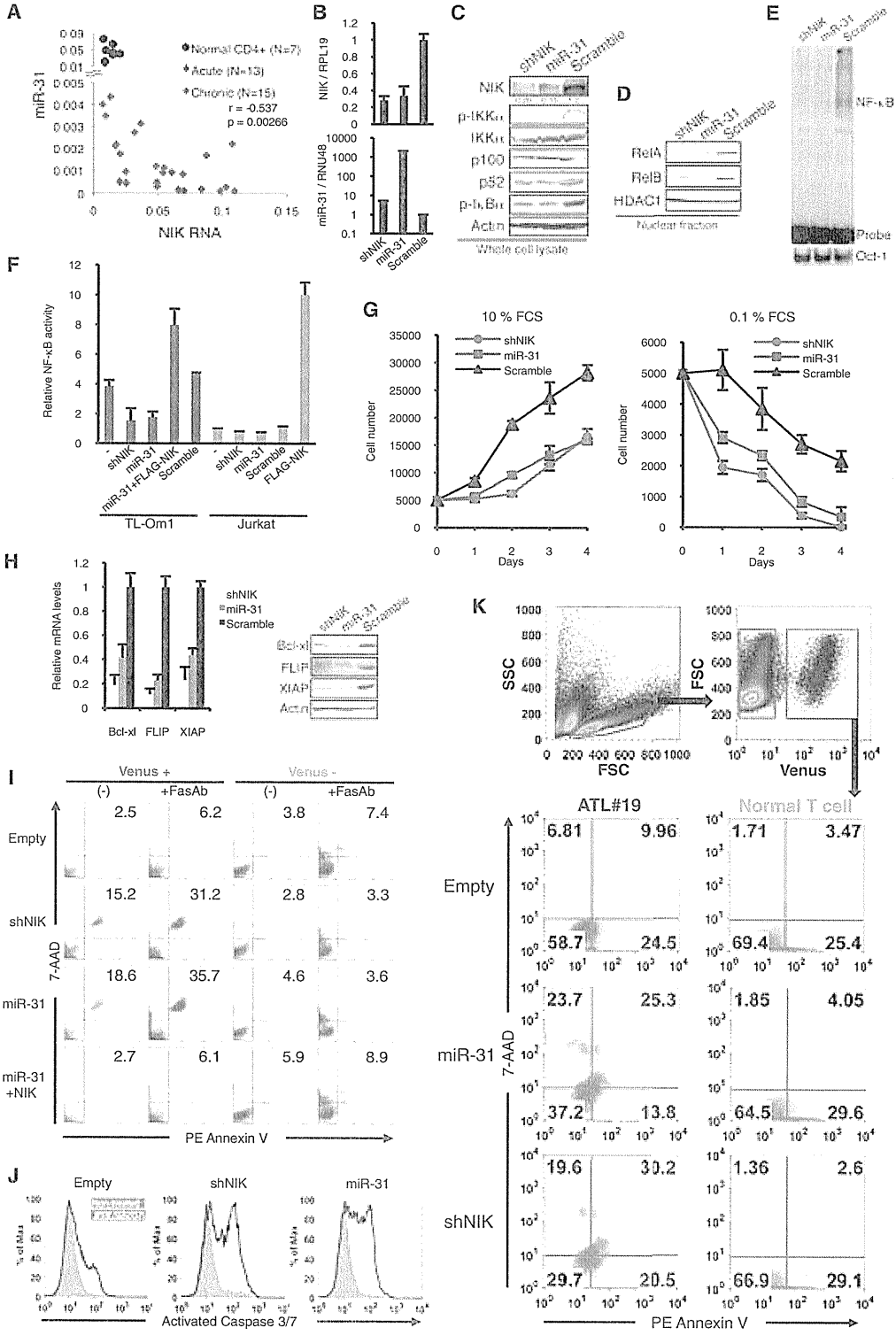

Figure 3. Loss of miR-31 Is Responsible for Constitutive NF-κB Activation, Abnormal Cell Growth, and Resistance to Apoptotic Cell Death in ATL Cells

(A) Expression levels of miR-31 and *NIK* in individual ATL patients and normal controls using data set obtained by quantitative RT-PCR. Pearson's correlation coefficient within ATL samples was described in the graph.

adjacent to clusters of the *CDKN2* and *IFNA* families, and is a well-known hotspot of genomic loss in several types of human cancers. We performed genome-wide scans of genetic lesions in 168 ATL samples and demonstrated that 21 ATL cases (12.5%) had genomic deletion of 9p21.3 containing the *hsa-miR-31* coding region (Figure 4A; Figure S3A). All of these cases also have genomic defect in *CDKN2A* region. A major proportion of ATL cases that are without genetic deletion and somatic mutation in the *hsa-miR-31* region showed remarkable loss of miR-31 expression (Figure 4B). Detailed expression profiling revealed drastic downregulation of *Pri-miR-31* transcription in the primary ATL cells (Figure 4C). There was a strong correlation between the levels of mature miR-31 and primary transcript ($r = 0.9414$, $p = 5.45 \times 10^{-8}$). *hsa-miR-31* is located in intronic region of *LOC554202* gene. However, *LOC554202* mRNA levels were very low in primary T cells and there was no significant difference between ATL and normal cells, strongly suggesting that loss of miR-31 expression is due to specific transcriptional suppression in ATL cells. Using computational analysis, we identified a putative TATA box and transcriptional start site (TSS) 2500 bp upstream of the miR-31 coding region (Figure 4D). Although no CpG islands were found in this region, we unexpectedly discovered an assembly of YY1-binding motifs upstream of the miR-31 region in human and mouse (Figure 4D; Figure S3C). YY1 is a pivotal transcription factor and a recruitor of the Polycomb repressive complex (PRC) (Simon and Kingston, 2009). Convergence of the YY1 binding sequence, especially the repressive motif (Figure S3D), seems to be evolutionarily conserved, suggesting that YY1 is important in the regulation of miR-31 transcription. We further performed chromatin immunoprecipitation (ChIP) to evaluate repressive histone hallmarks, including di- and trimethylated H3K9 (H3K9me2 and H3K9me3) and trimethylated H3K27 (H3K27me3). The results showed higher levels of methylation at H3K9 and H3K27 in a broad area containing the miR-31 coding region (Figure 4E). As shown in Figures S3E–S3G, there was an inverse correlation between the levels of miR-31 expression and repressive histone methylation. These data allowed us to hypothesize that histone methylation, especially that of Polycomb family-dependent H3K27me3, may contribute to miR-31 repression. To confirm our hypothesis, we performed a YY1 knockdown experiment using a specific shRNA (Figures 4F–4I). As expected, knockdown of YY1 led to an increase in the levels of *Pri-miR-31* and mature miR-31 (Figures 4F and 4G). Furthermore, ChIP assays showed that YY1 occupied the miR-31 region, especially in the upstream region of TSS, where there is an array of YY1 binding sites (Figures 4D and 4H). The results also demonstrated that decreased occupancy of YY1 and concomitant derecruitment of EZH2, a key component of PRC2, were induced by YY1 knockdown, indicating involvement of EZH2 in the repressive complex recruited to the miR-31 region (Figures 4H and 4I; Figure S3H). These results collectively suggest that YY1 regulates PRC2 localization and initiates miR-31 suppression. Indeed, we found significant escalation of methylated histone H3K9 and H3K27 at the miR-31 locus of peripheral blood lymphocytes of ATL patients (Figure 4J), indicating that aberrant abundance of suppressive histone methylation may be responsible for the loss of miR-31 in the primary ATL cells.

Overexpression of PRC2 Components Leads to miR-31 Repression

Given that Polycomb-mediated repressiveness affects miR-31 level, our findings imply that the amount of EZH2 is related to miR-31 expression (Figure 4I; Figures S3G and S4A). We found a significantly upregulated expression of PRC2 components, especially EZH2 and SUZ12, in the primary ATL cells (Figures 5A and 5B; Table S3). Quantitative RT-PCR revealed that miR-31 levels inversely correlated with both *EZH2* and *SUZ12*, respectively (Figure 5C). miR-101 and miR-26a, which are putative negative regulators of EZH2, seem to be associated with this relationship in ATL cells (Figures S4B–S4E). To further confirm our hypothetical mechanism linking the epigenetic machinery and miR-31 expression, we performed a "loss-of-PRC2-function" assay. Retroviral delivery of shSUZ12 and shEZH2 in the ATL cell lines resulted in a great increase in the levels of *Pri-miR-31* and its mature form (Figure 5D; Figure S4F). Knockdown of PRC2 induced histone demethylation at H3K27 in the miR-31 region, which is concomitant with the decrease in H3K9me3 levels, EZH2 occupancy, and HDAC1 recruitment (Figure 5E), suggesting that this multimeric complex leads to a completely closed chromatin architecture as a result of histone modifications in the miR-31 genomic region.

To further examine whether the proposed mechanism holds true in other human cancers, we analyzed a couple of carcinoma cell lines, including HeLa cells and nonmetastatic and metastatic breast carcinoma cell lines, MCF7 and MDA-MB-453 cells, respectively. qRT-PCR revealed that expression of *EZH2* and *SUZ12* inversely correlated with miR-31 levels (Figure S4G).

(B) miR-31 restoration by retroviral vector inhibits *NIK* RNA accumulation in TL-Om1 cells. The results of *NIK* and mature miR-31 quantifications are shown (n = 3, mean ± SD).
(C) miR-31 or shNIK expression downregulates NIK protein expression and inhibits downstream pathway of noncanonical NF-κB in TL-Om1 cells.
(D) Reduced nuclear translocation of RelA and RelB proteins in miR-31- or shNIK-expressing TL-Om1 cells.
(E) miR-31-dependent downregulation of NF-κB activity in TL-Om1 cells examined by EMSA.
(F) NF-κB-luciferase reporter assays (n = 5, mean ± SD). FLAG-NIK plasmid was transiently introduced 48 hr prior to the assay.
(G) miR-31 level is relevant to proliferation of ATL cells. Cell proliferation curve of TL-Om1 cells were evaluated in two FCS conditions (n = 3, mean ± SD).
(H) Apoptosis-related gene expression in TL-Om1 cells analyzed by qRT-PCR (n = 3, mean ± SD) and western blots.
(I) Lentivirus-mediated NIK depletion promotes basal and Fas antibody-mediated apoptosis. Venus-positive population represented lentivirus-infected cells. Apoptotic cells were determined by PE-Annexin V / 7-AAD stainings (n = 4). Representative FACS analyses are shown.
(J) miR-31 activates Caspase 3/7 determined by FACS (n = 3).
(K) miR-31 expression and NIK depletion induce tumor cell death. Primary tumor cell from ATL patient and healthy CD3+ T cells were infected with lentivirus and analyzed by FACS. The apoptotic cells were defined by sequential gating beginning with FSC-SSC to select intact lymphocytes, subgating on the Venus-positive population, and calculating the PE-Annexin V and 7-AAD profilings. Representative result is shown and summarized data are presented in Figure 6J. See also Figure S2.

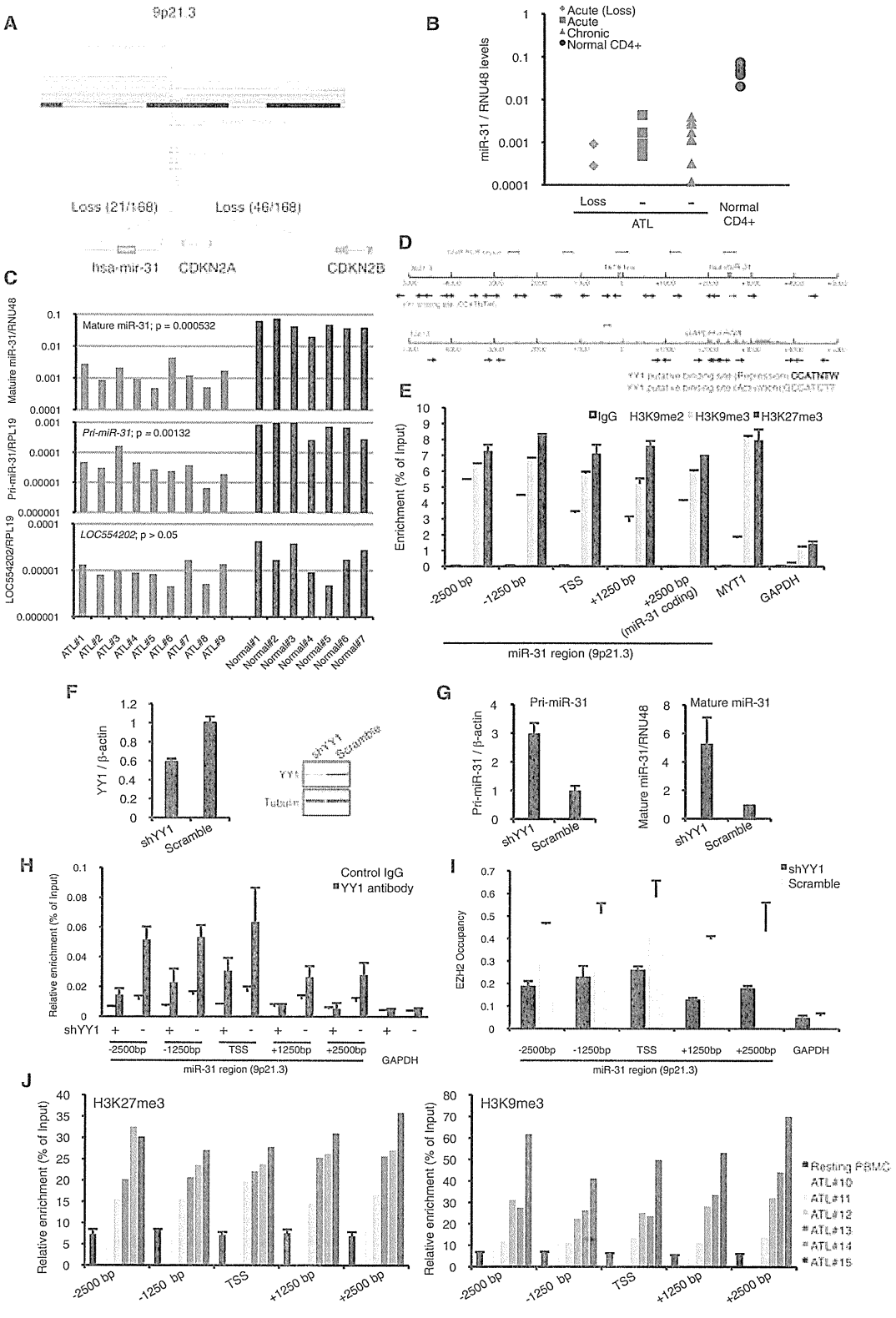
A
9p21.3
Loss (21/168)
Loss (46/168)
hsa-mir-31
CDKN2A
CDKN2B
B
Acute (Loss)
Acute
Chronic
Normal CD4+
miR-31 / RNU48 levels
Loss
ATL
Normal CD4+
C
Mature miR-31; p = 0.000532
Pri-miR-31; p = 0.00132
LOC554202; p > 0.05
Mature miR-31/RNU48
Pri-miR-31/RPL19
LOC554202/RPL19
ATL#1 ATL#2 ATL#3 ATL#4 ATL#5 ATL#6 ATL#7 ATL#8 ATL#9
Normal#1 Normal#2 Normal#3 Normal#4 Normal#5 Normal#6 Normal#7
D
E
IgG H3K9me2 H3K9me3 H3K27me3
Enrichment (% of Input)
-2500 bp
-1250 bp
TSS
+1250 bp
+2500 bp (miR-31 coding)
MYT1
GAPDH
miR-31 region (9p21.3)
F
YY1 / β-actin
shYY1
Scramble
YY1
Tubulin
G
Pri-miR-31
Pri-miR-31 / β-actin
Mature miR-31
Mature miR-31/RNU48
H
Control IgG
YY1 antibody
Relative enrichment (% of Input)
shYY1
-2500bp
-1250bp
TSS
+1250bp
+2500bp
GAPDH
miR-31 region (9p21.3)
I
shYY1
Scramble
EZH2 Occupancy
J
H3K27me3
H3K9me3
Relative enrichment (% of Input)
Resting PBMC
ATL#10
ATL#11
ATL#12
ATL#13
ATL#14
ATL#15

ChIP assays detected higher levels of trimethylated H3K27 and EZH2 occupancy in cells showing lower expression levels of miR-31 (Figure S4H). Furthermore, knockdown of EZH2 or SUZ12 restored miR-31 transcription in MDA-MB-453 and MCF7 cells (Figures 5F and 5G; Figure S4K, respectively), which are consistent with the results obtained with ATL cells. These results indicate a link between Polycomb-mediated epigenetic regulation and miR-31 transcription in ATL and breast cancer cell lines.

Polycomb Group Regulates NF-κB Pathway by Controlling miR-31 Expression

Based on our findings, we considered an aspect of the biological communication between epigenetic silencing and the NF-κB pathway through miR-31 regulation. The microarray data sets showed positive correlations between PRC2 components and miR-31 target gene, *NIK* expression (Figure 6A). The results also suggested that these factors tend to show higher levels in the aggressive subtype (acute type) than in the indolent subtypes (chronic and smoldering types), implying that these genes may play important roles in the clinical phenotype and prognosis of ATL. To examine this notion, we performed PRC2 knockdown in ATL cell lines. Western blots of these cells demonstrated decreased levels of NIK, p52, and phospho-IκBα (Figure 6B; Figure S5A), suggesting suppression of both canonical and noncanonical NF-κB cascade and activity (Figure 6C; Figures S5B and S5C). These results are consistent with those of miR-31 overexpression (Figures 3C–3F). Then, we tested whether exogenous manipulation of miR-31 could restore the effect of PRC2 loss. Anti-miR-31 treatment rescued impaired NF-κB activity in PRC2-disrupted cells (Figure 6D). On the other hand, overexpression of EZH2 induced NF-κB activation, which was partially canceled by the introduction of miR-31 precursor (Figure 6E; Figure S5D). These results suggest that Polycomb-mediated miR-31 suppression leads to NF-κB activation. Indeed, knockdown of the PRC2 complex led to reduced levels of cell proliferation and greater sensitivity to serum deprivation in ATL cells (Figure 6F; Figure S5E). In addition, PRC2 disruption showed a reduction in cell migration (Figure S5F).

To gain further insight into this general network, we studied the functions of miR-31 and the PRC2 complex in breast cancer cell lines. NF-κB activity was downregulated by knockdown of PRC2 components in MDA-MB-453 cells (Figure 6G; Figures S5G and S5H), although no significant differences were observed in cell proliferation (data not shown). Repression of NF-κB activity induced by knockdown of PRC2 components was partially restored by treatment with a miR-31 inhibitor, suggesting that PRC2 knockdown-mediated relief of NF-κB repression is at least a part of the result of the miR-31 induction. In addition, knockdown of PRC2 components resulted in a reduced level of receptor-initiated accumulation of NIK in B cells (Figure 6H). Our findings indicate a common molecular mechanism comprising Polycomb-mediated epigenetic regulation, miR-31 expression and the NF-κB signaling pathway.

Regulation of NF-κB by Polycomb family may in turn control the cellular apoptosis responses. We found that lentivirus-mediated EZH2 knockdown led to increased apoptotic sensitivity in TL-Om1 cells (Figure 6I). Additional expression of NIK inhibited the cell death induced by EZH2 knockdown, suggesting the reciprocal relationship between Polycomb and NF-κB cascades. By using primary tumor cells from patient, we tested the killing effect induced by miR-31, NIK knockdown, and EZH2 knockdown (Figure 6J; Figures S5I and S5J). All tested samples showed strong death response, demonstrating that survival of ATL cells was closely associated with miR-31, NIK, and EZH2, all of which show deregulated expression in ATL cells.

By qRT-PCR we finally examined the expression levels of some genes involved in the noncanonical NF-κB pathway. As shown in Figure 6K, the results clearly demonstrated higher expression levels of positive regulators such as *NIK*, *CD40,* and *LTBR*, and lower expression levels of the negative regulators such as *BIRC2/3* (cIAP1/2), which are involved in proteasomal degradation of NIK (Zarnegar et al., 2008a). These observations are in line with a previous report on Multiple Myeloma cells (Annunziata et al., 2007). In addition to these data, we obtained convincing evidence for a molecular aspect of NIK accumulation in ATL cells. Polycomb-dependent epigenetic gene silencing may be associated with miR-31 loss, followed by NF-κB activation and other signaling pathways (Figure 7).

DISCUSSION

Constitutive activation of NF-κB contributes to abnormal proliferation and inhibition of apoptotic cell death in cancer cells,

Figure 4. Genetic and Epigenetic Abnormalities Cause miR-31 Loss in ATL Cells

(A) Genomic loss of chromosome 9p21.3 in primary ATL cells. Copy number analyses revealed tumor-associated deletion of miR-31 region (21/168) and *CDKN2* region (46/168). Recurrent genetic changes are depicted by horizontal lines based on CNAG output of the SNP array analysis.

(B) miR-31 expression in various sample sets. Expression levels were evaluated by real-time PCR.

Loss, samples with genomic loss of the miR-31 region; (–) samples without genomic loss of the miR-31 region.

(C) PCR-based miR-31 quantifications in primary ATL samples. ATL samples without genetic loss in miR-31 region (n = 9, Figure S3B), and normal CD4+ T cells (n = 7) were tested. p values (ATL versus normal) are shown.

(D) YY1 binding motif cluster around transcriptional start site (TSS) of miR-31 region. Arrows represent positions of the motifs. Regions of PCR amplification for ChIP assay are shown.

(E) Repression-associated histone methylation in miR-31 region determined by ChIP assay (n = 3, mean ± SD). The results of relative enrichment against input control are presented and distance from miR-31 TSS is described. *MYT1* and *GAPDH* promoters are as positive or negative controls, respectively.

(F–I) YY1-dependent EZH2 occupancy in miR-31 locus. (F) YY1 knockdown in TL-Om1 cells. qRT-PCR (left, n = 3, mean ± SD) and western blotting (right) showed decreased YY1 level. (G) YY1 knockdown led to both primary and mature miR-31 restoration in TL-Om1 cells (n = 3, mean ± SD). (H) YY1 occupancy in miR-31 region analyzed by ChIP (n = 3, mean ± SD). YY1 occupancy in miR-31 locus was reduced by YY1 knockdown. (I) EZH2 occupancy in miR-31 region analyzed by ChIP (n = 3, mean ± SD). YY1 knockdown inhibited EZH2 recruitment in miR-31 region.

(J) Aberrant accumulation of repression-associated histone methylations widely in miR-31 region of primary ATL cells. PBMCs freshly isolated from ATL patients (n = 6) were analyzed by ChIP assay. PBMC from healthy adults were used for normal controls. See also Figure S3.

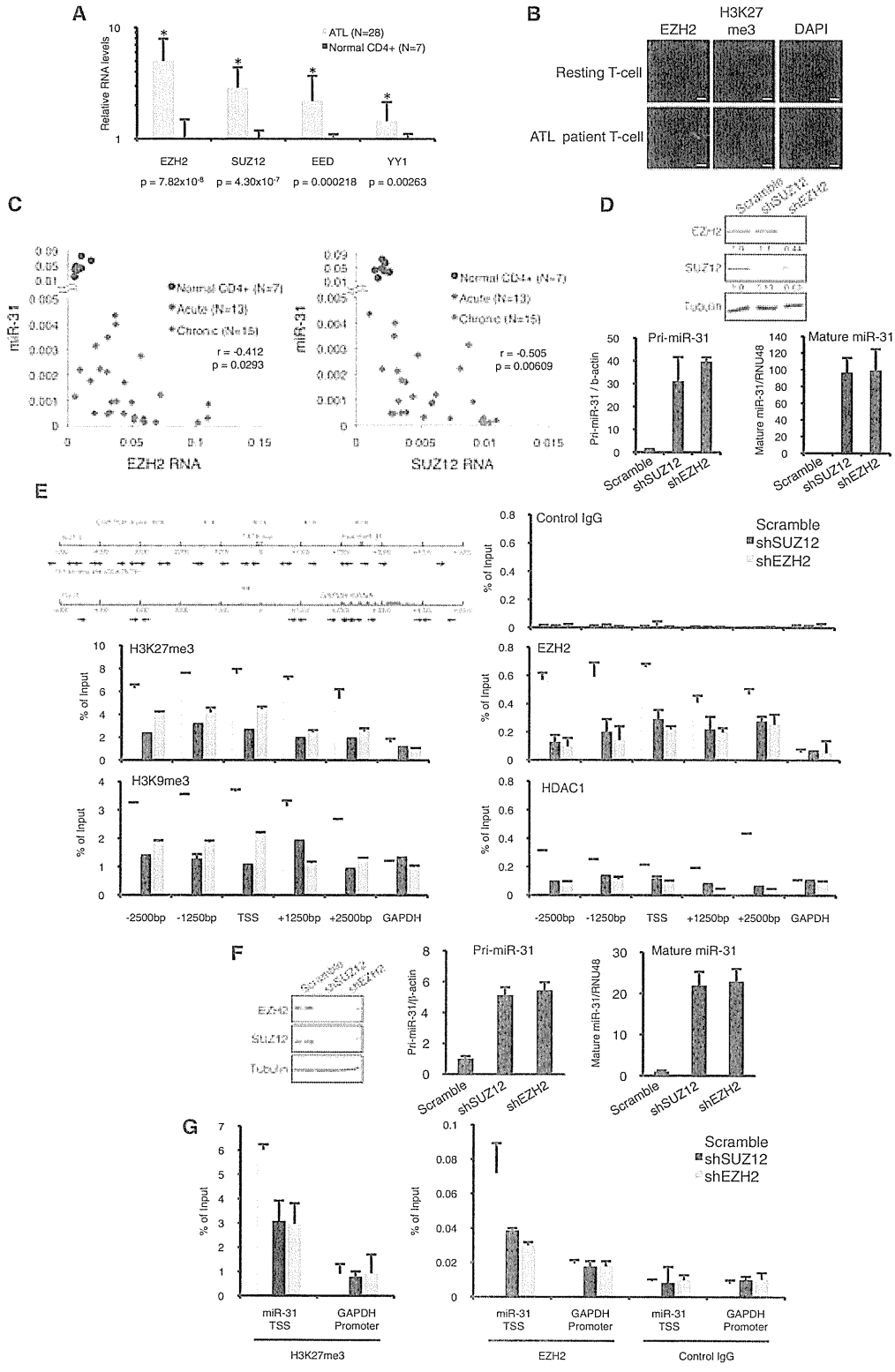
A
ATL (N=28)
Normal CD4+ (N=7)
Relative RNA levels
EZH2
SUZ12
EED
YY1
p = 7.82x10-8
p = 4.30x10-7
p = 0.000218
p = 0.00263
B
H3K27 me3
EZH2
DAPI
Resting T-cell
ATL patient T-cell
C
miR-31
Normal CD4+ (N=7)
Acute (N=13)
Chronic (N=15)
r = -0.412
p = 0.0293
EZH2 RNA
r = -0.505
p = 0.00609
SUZ12 RNA
D
Scramble
shSUZ12
shEZH2
EZH2
SUZ12
Tubulin
Pri-miR-31
Pri-miR-31 / b-actin
Mature miR-31
Mature miR-31/RNU48
E
Control IgG
Scramble
shSUZ12
shEZH2
% of Input
H3K27me3
EZH2
H3K9me3
HDAC1
-2500bp
-1250bp
TSS
+1250bp
+2500bp
GAPDH
F
Pri-miR-31
Mature miR-31
G
miR-31 TSS
GAPDH Promoter
H3K27me3
EZH2
Control IgG

including ATL, diffuse large B cell lymphoma (DLBCL), Hodgkin lymphoma, breast cancer, prostate cancer and others (Prasad et al., 2010). NF-κB is also essential for various cell functions, including inflammation, innate immunity, and lymphocytic development (Hayden and Ghosh, 2008). Identification of NF-κB determinants will lead to marked progress in understanding molecular pathology.

Our global analyses demonstrated an interesting miRNA expression signature as well as an aberrant mRNA expression profile, which may be associated with leukemogenesis in the primary ATL cells (Figures 1 and 6A). We revealed downregulation of tumor-suppressive miRNA including Let-7 family, miR-125b, and miR-146b, which can contribute to aberrant tumor cell signaling. Recent studies have suggested unique expression profiles of miRNAs in ATL (Yeung et al., 2008; Bellon et al., 2009), but loss of miR-31 has not been focused. Cellular amount of miRNAs may be susceptible to various environments such as transcriptional activity, maturation processing, and also epigenetic regulation. The end results appear to be affected by methodology employed and conditions and types of samples used. Our integrated expression profiling of primary ATL cells are based on a significantly larger number of samples and fruitfully provides intriguing information that may be useful in improving the understanding of T cell biology as well as in the identification of biomarkers for diagnosis.

Pleiotropy of miR-31 was first reported by Valastyan et al. (2009). The authors elegantly demonstrated the function of miR-31 in vivo and also identified several target genes that contribute to cell migration and invasiveness. In the present study, we focused on the functional significance of miR-31 in the regulation of NF-κB signaling that contributes to tumor cell survival.

Overexpression of NIK acts as an oncogenic driver in various cancers. In the present study, NIK was identified as a miR-31 target based on several lines of evidence. First, luciferase-3′ UTR reporter assay showed that *NIK* 3′ UTR sequence has a role for negative regulation (Figure S1B). By combining a specific inhibitor and mutations in miR-31-binding site, we demonstrated that miR-31 recognizes and negatively regulates the *NIK* 3′ UTR (Figures 2A and 2D). Second, by introducing a miR-31 precursor or inhibitor, we showed that amount of miR-31 inversely correlates with levels of NIK expression and downstream signaling (Figures 2E–2K). Third, genetic evidence indicated strong base pairing and biological conservation (Bartel, 2009) (Figures S1L–S1O). Our experimental approach illustrated that mmu-miR-31 regulates mouse *Map3k14* gene. Fourth, individual assessments using gene expression data clearly revealed an inverse correlation between the expression levels of miR-31 and *NIK* (Figure 3A). Collectively, we provide definitive evidence for the notion that miR-31 negatively regulates NIK expression and activity.

It is well known that the NIK level directly regulates NF-κB activity in various cell types (Thu and Richmond, 2010). We experimentally showed that miR-31 regulates noncanonical NF-κB activation stimulated by BAFF and CD40L, both of which are major B cell activating cytokines. Since signals from receptors are essential for the development and activity of B cells, the negative role of miR-31 in cytokines-induced NIK accumulation appears to be widely important in the noncanonical regulation of NF-κB in B cells and other cell types (Figures 2H–2K). Again, our findings revealed the role of NIK in the regulation of canonical NF-κB pathway. Strict regulation of NIK appears to be closely associated with the fate of lymphocytes.

The level of miR-31 was drastically suppressed in all tested primary ATL cells, and its magnitude is greater than that which has been reported in other cancers. Our results demonstrated a profound downregulation of miR-31 (fold change, 0.00403; Figure 1B) in all ATL cases, suggesting that miR-31 loss is a prerequisite for ATL development. Restoration of miR-31-repressed NF-κB activity in ATL cells, resulting in impairment of the proliferative index and apoptosis resistance (Figure 3). Furthermore, our results demonstrate that inhibition of NF-κB promotes tumor cell death in cell lines and also primary tumor cells from ATL patients (Figures 3 and 6), which are consistent with our previous observation (Watanabe et al., 2005). Since it is highly possible that miR-31 and relevant factors are pivotal in cancers, their expressions would have a great importance in view of biomarkers for the aberrant signaling and clinical outcomes.

By studying clinical samples and in vitro and ex vivo models, we obtained several biologically interesting results. First, we identified the Polycomb protein complex as a strong suppressor of miR-31. Generally, the Polycomb group constitutes a multimeric complex that negatively controls a large number of genes involved in cellular development, reproduction, and stemness (Sparmann and van Lohuizen et al., 2006). However, the key molecules involved in cancer development, progression, and prognosis are not yet fully understood. In breast and prostate cancers, oncogenic functions of EZH2 and NF-κB activation were reported independently (Kleer et al., 2003; Varambally et al., 2002; Suh and Rabson, 2004). Interestingly, these tumors show low miR-31 levels (Valastyan et al., 2009; Schaefer et al., 2010). Recently, Min et al. (2010) reported that EZH2 activates NF-κB by silencing the DAB2IP gene in prostate cancer cells.

Figure 5. Amount of PRC2 Components Epigenetically Links to miR-31 Expression in T Cells and Epithelial Cells

(A) Overexpression of PRC2 components in primary ATL cells measured by qRT-PCR (ATL, n = 28; normal, n = 7; mean ± SD). These results were supported by the data of gene expression microarray (Table S3).

(B) Escalation of EZH2 protein and trimethylated H3K27 levels in primary ATL cells illustrated by immunocytostaining (n = 4, a representative result is shown). Resting T cells were as normal control. Scale bars = 20 μm.

(C) Statistical correlation among the levels of miR-31, *EZH2*, and *SUZ12* in individual ATL samples. Correlation coefficients within ATL samples are shown in the graphs.

(D and E) Loss of PCR2 function causes chromatin rearrangement and miR-31 upregulation. (D) TL-Om1 cells expressing shSUZ12, shEZH2, and scrambled RNA were established by retroviral vector. The levels of EZH2, SUZ12, *Pri-miR-31*, and mature miR-31 were measured by western blotting and qRT-PCR (n = 3, mean ± SD). (E) Results of ChIP assays with indicated antibodies (n = 3, mean ± SD). Amounts of immunoprecipitated DNA were analyzed by region-specific PCR. *GAPDH* promoter served as a region control.

(F and G) Knockdown of Polycomb family proteins in MDA-MB-453 cells. (F) EZH2 and SUZ12 are shown by western blot. miR-31 level was examined by qRT-PCR (n = 3, mean ± SD). (G) Histone methylation and EZH2 occupancy evaluated by ChIP assay (n = 3, mean ± SD). See also Table S3 and Figure S4.

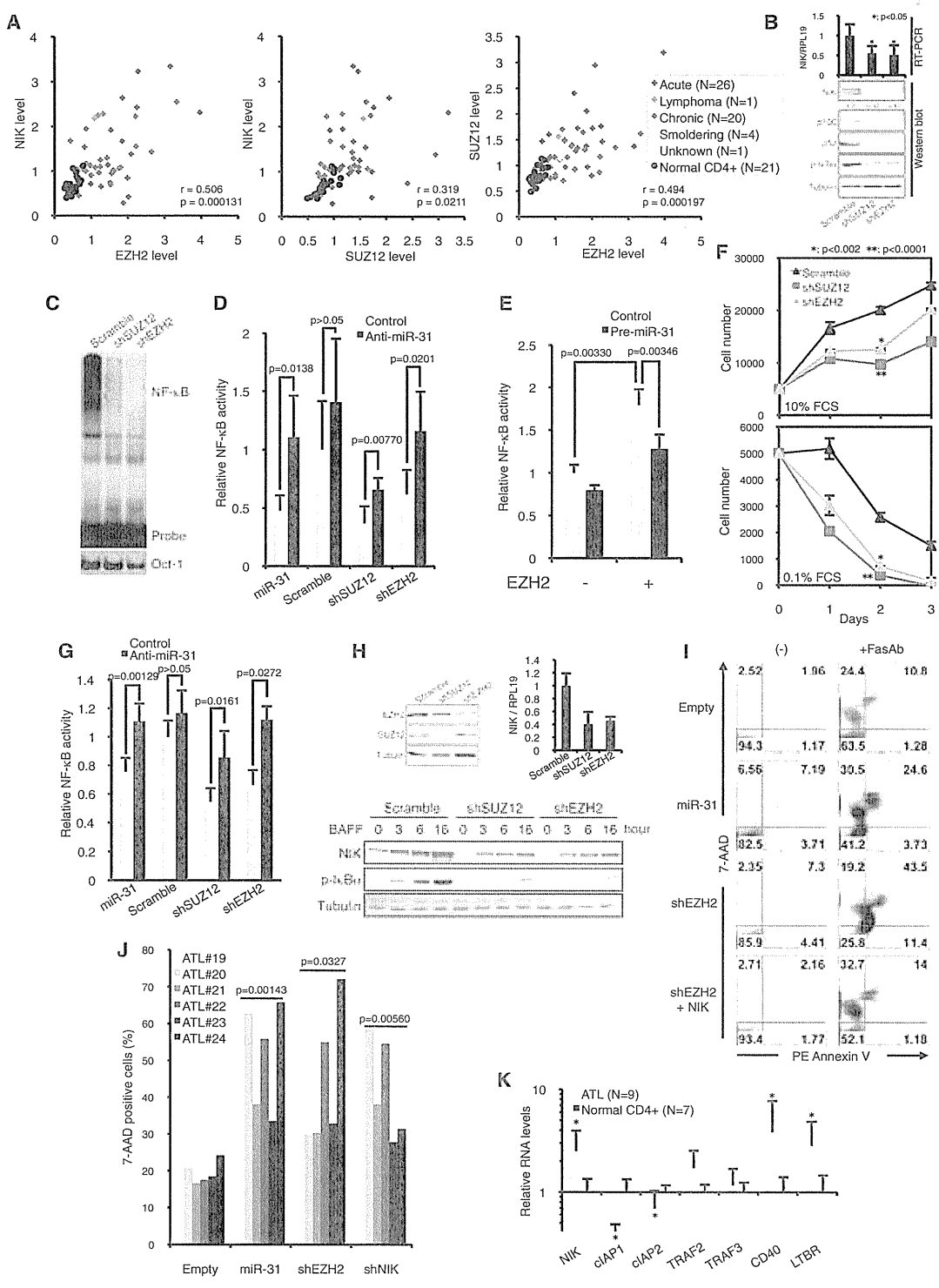

Figure 6. Epigenetic Change Driven by Polycomb Group Mediates NF-κB Signaling through miR-31 Regulation

(A) Reciprocal relationship of mRNA expression between *NIK* and Polycomb group in primary samples. Pearson's correlation coefficients among ATL samples are shown.

(B) PRC2 knockdown negatively affects NF-κB signaling in TL-Om1 cells. After establishment of PRC2 knockdown, the levels of *NIK* RNA (n = 4, mean ± SD) and proteins of NIK, p52/p100, and phospho-IκBα were examined.

(C) Downregulation of NF-κB activity in PRC2-disrupted cells detected by EMSA.

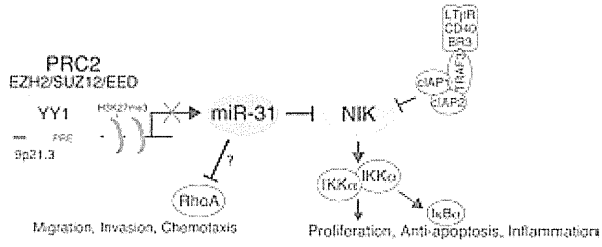

Figure 7. Proposed Model for ATL and Other Tumor Cells
Polycomb repressive factors are linked to NIK-dependent NF-κB activation via miR-31 regulation.

In the present study, we found that the Polycomb group regulates miR-31 expression and that elevated expression of EZH2 leads to NF-κB activation via NIK-miR-31 regulation in ATL and breast cancer cells (Figure 6). We also showed that restoration of miR-31 partially impaired Polycomb-mediated NF-κB operation (Figures 6D, 6E, and 6G), suggesting that miR-31 is involved in this relationship. Furthermore, a connection between NIK and PRC2 was observed in B cells (Figure 6H). Polycomb group proteins are essential in lymphocyte development and activation (Su et al., 2003, 2005). Further, given the NF-κB is a pivotal transcription regulator in normal and oncogenic functions, practical participations of epigenetic regulators and miR-31 in NF-κB signaling will increase our understanding of the molecular mechanisms of T cell functions. For generalization of the molecular axis in other cancers and normal cells, further study will be needed.

Second, YY1 is a recruiter of PRC2 to the miR-31 region. In humans, the Polycomb response element (PRE) has not been precisely identified. A good candidate for a mammalian recruiter of PRC2 is YY1, the homolog of *D. melanogaster* PHO (Simon and Kingston, 2009). We found an assembly of the YY1 binding motif in the miR-31 locus and demonstrated that YY1 knockdown dislodged EZH2 in this region (Figure 4I), which supports previous findings (Caretti et al., 2004). The detailed mechanism by which YY1 mediates recruitment of the Polycomb family may be important in the context of epigenetic regulation of orchestrated gene expression and T cell functions.

Third, Polycomb family proteins can control miRNA expression in an epigenetic fashion. The amount of PRC2 factors strongly influenced the degree of suppression of miR-31 expression (Figure 5). We speculate that, in addition to controlling the transcription, the Polycomb group can modulate translation via miRNA regulation. Furthermore, miR-101 and miR-26a are known to regulate EZH2 expression (Sander et al., 2008; Varambally et al., 2008), which is supported by our observation (Figure S4C). This signaling circuit will permit multiple gene regulation. Whereas genetic loss at the miR-31 locus is observed in some cases of ATL (Figure 4A), no genetic deletion in the miR-101-1 or miR-101-2 region was detected in ATL, which is not consistent with a previous finding in prostate cancer. Our results also suggested putative association between Let-7 family and EZH2 (Figure S4). Aberrant downregulations of these miRNAs in the primary ATL cells will be the next important questions to be addressed in efforts to improve understanding of the oncogenic signaling network.

By collaborative profiling of miRNA and mRNA expression, we identified a notable relationship between ATL subtypes and a gene cluster that contains miR-31, NIK, EZH2, and SUZ12. This finding suggests that an aberrant gene expression pattern correlates with the malignant phenotype, and this provides important clues about clinical manifestations and may help identify therapeutic targets against ATL cells (Figure 6A). Although HDAC inhibitors did not show effective responses (Figures S4I and S4J), emerging epigenetic drug such an EZH2 inhibitor (Fiskus et al., 2009) may pave a pathway leading to cures for various malignancies that involve constitutive activation of NF-κB.

In summary, we show that genetic and epigenetic loss of miR-31 is responsible for oncogenic NF-κB activation and malignant phenotypes in ATL. This provides evidence for the idea that miR-31 is an important tumor suppressor. An emerging pathway involving an epigenetic process, miR-31, and NF-κB will provide a conceptual advance in epigenetic reprogramming, inflammatory signaling, and oncogenic addiction.

EXPERIMENTAL PROCEDURES

Cell Lines and Primary ATL Cells

The primary peripheral blood mononuclear cells (PBMCs) from ATL patients and healthy volunteers used in the present work were a part of those collected with an informed consent as a collaborative project of the Joint Study on Prognostic Factors of ATL Development (JSPFAD). The project was approved by the Institute of Medical Sciences, the University of Tokyo (IMSUT) Human Genome Research Ethics Committee. Additional ATL clinical samples for copy number analysis were provided by Drs. Y. Yamada, Nagasaki University,

(D) NF-κB activity evaluated by reporter assays in the presence or absence of miR-31 inhibitor (n = 5, mean ± SD). Anti-miR-31 treatment partially rescued the NF-κB activity in PRC2 knockdowned TL-Om1 cells.
(E) Overexpressed EZH2 activates NF-κB via miR-31. Jurkat cells were transfected with an EZH2 plasmid together with miR-31 precursor or control RNA (n = 5, mean ± SD).
(F) PRC2 dysfunction changes TL-Om1 cell proliferation and response to serum starvation. Under conditions of 10% or 0.1% of FCS, cell growth curves were examined (n = 3, mean ± SD). PRC2 downregulation decreased cell growth with statistical significance.
(G) NF-κB activity in PRC2-knockdowned MDA-MB-453 cells in the presence or absence of miR-31 inhibitor were examined (n = 5, mean ± SD).
(H) PRC2 disruption inhibits BAFF-dependent NIK accumulation and IκBα phosphorylation in BJAB cells.
(I) Apoptotic cell death induced by lentivirus-mediated EZH2 knockdown in TL-Om1. Venus-positive populations were analyzed by Annexin V/7-AAD stainings (n = 3) and representative of FACS data are shown.
(J) Summary of primary tumor cell death. Lentivirus-based miR-31 expression, NIK knockdown, and EZH2 knockdown showed killing effects in six primary ATL samples. Statistical significances are shown in the graph. Results of FACS and qRT-PCR are shown in Figures S5I and S5J.
(K) Expression levels of genes involved in noncanonical NF-κB pathway in primary ATL cells (ATL, n = 9; normal, n = 7; mean ± SD). Relative expression levels were tested by qRT-PCR (*$p < 0.05$). See also Figure S5.

and K. Ohshima, Kurume University, where the projects were approved by the Research Ethics Committees of Nagasaki University and Kurume University, respectively. PBMC were isolated by Ficoll separation. ATL cells, primary lymphocytes, and all T cell lines were maintained in RPMI1640 supplemented with 10% of FCS and antibiotics. Clinical information of ATL samples is provided in Table S1.

Expression Analyses

Clinical samples for microarrays were collected by a collaborative study group, JSPFAD (Iwanaga et al., 2010). Gene expression microarray was used 4x44K Whole Human Genome Oligo Microarray (Agilent Technologies) and miRNA microarray was used Human miRNA microarray kit v2 (Agilent Technologies), respectively. Quantitative RT-PCR was performed with SYBRGreen (TAKARA). Mature miRNA assays were purchased from Applied Biosystems.

Copy Number Analyses

Genomic DNA from ATL patients was provided from the material bank of JSPFAD, Nagasaki University, and Kurume University, and was analyzed by Affymetrix GeneChip Human Mapping 250K Nsp Array (Affymetrix). Obtained data were analyzed by CNAG/AsCNAR program (Chen et al., 2008).

Oligonucleotides, Plasmids, and Retrovirus Vectors

All RT-PCR primers and oligonucleotides are described in Supplemental Experimental Procedures. miRNA precursor and inhibitor were from Applied Biosystems. Transfection of small RNA and other plasmid DNA were performed by Lipofectamine2000 (Invitrogen). For miRNA or shRNA expression, retroviral vectors (pSINsi-U6, TAKARA) were used.

3′ UTR-Conjugated miR-31 Reporter Assay

HeLa cells were cotransfected with 3′ UTR-inserted pMIR-REPORT firefly plasmid (Ambion), RSV-Renilla luciferase plasmid, and miRNA inhibitor. The cells were collected at 24 hr posttransfection, and Dual-luciferase reporter assay was performed (Promega).

Analysis of NF-κB Pathway

NF-κB activity was evaluated by EMSA and reporter assays as previously described (Horie et al., 2004). Antibodies for western blots are described in supplemental information. Cell proliferative assay was performed by Cell Counting Kit-8 (Dojindo).

Lentivirus Vectors and Apoptosis Analysis

A lentivirus vector (CS-H1-EVBsd) was provided from RIKEN, BRC, Japan. Lentivirus solution was produced by cotransfection with packaging plasmid (pCAG-HIVgp) and VSV-G- and Rev-expressing plasmid (pCMV-VSV-G-RSV-Rev) into 293FT cells. After infection of lentivirus, the apoptotic cell was evaluated by PE Annexin V / 7-AAD staining (BD PharMingen) and analyzed by FACS Calibur (Becton, Dickinson). Collected data were analyzed by FlowJo software (Tree Star).

ChIP Assay

ChIP assay was previously described (Yamagishi et al., 2009). Briefly, cells were crosslinked with 1% of formaldehyde, sonicated, and subjected to chromatin-conjugated IP using specific antibodies. Precipitated DNA was purified and analyzed by real-time PCR with specific primers (see Supplemental Experimental Procedures).

Computational Prediction

To identify miR-31 target genes, we integrated the output results of multiple prediction programs; TargetScan, PicTar, miRanda, and PITA. RNAhybrid was for secondary structure of miRNA-3′ UTR hybrid. TSSG program was for TATA box and TSS predictions. DNA methylation site was predicted by CpG island Searcher.

Statistical Analyses

Data were analyzed as follows: (1) Welch's t test for Gene Expression Microarray (p value cutoff at 10^{-6}) and miRNA Microarray (p value cutoff at 10^{-5}); (2) Pearson's correlation for two-dimensional hierarchical clustering analysis and individual assessment of microarray data sets; (3) two-tailed pared Student's t test with $p < 0.05$ considered statistically significant for in vitro cell lines and primary cells experiments, including luciferase assay, RT-PCR, ChIP assay, cell growth assay, and migration assay. Data are presented as mean ± SD.

ACCESSION NUMBERS

Coordinates have been deposited in Gene Expression Omnibus database with accession numbers, GSE31629 (miRNA microarray), GSE33615 (gene expression microarray), and GSE33602 (copy number analyses).

SUPPLEMENTAL INFORMATION

Supplemental Information includes three tables, five figures, and Supplemental Experimental Procedures and can be found with this article online at doi:10.1016/j.ccr.2011.12.015.

ACKNOWLEDGMENTS

We thank Dr. M. Iwanaga, Mr. M. Nakashima, and Ms. T. Akashi for support and maintenance of JSPFAD. We thank Drs. H. Miyoshi and A. Miyawaki for providing the Venus-encoding lentivirus vectors. We also thank Dr. R. Horie for experimental advices, and Drs. T. Kanno and T. Ishida for providing the MDA-MB-453. Grant support: Grants-in-Aid for Scientific Research from Ministry of Education, Culture, Sports, Science, and Technology of Japan to T.W. (No. 23390250) and by Grants-in-Aid from the Ministry of Health, Labour and Welfare to T.W. (H21-G-002 and H22-AIDS-I-002).

Received: November 3, 2010
Revised: August 12, 2011
Accepted: December 19, 2011
Published: January 17, 2012

REFERENCES

Annunziata, C.M., Davis, R.E., Demchenko, Y., Bellamy, W., Gabrea, A., Zhan, F., Lenz, G., Hanamura, I., Wright, G., Xiao, W., et al. (2007). Frequent engagement of the classical and alternative NF-kappaB pathways by diverse genetic abnormalities in multiple myeloma. Cancer Cell *12*, 115–130.

Bartel, D.P. (2009). MicroRNAs: target recognition and regulatory functions. Cell *136*, 215–233.

Bellon, M., Lepelletier, Y., Hermine, O., and Nicot, C. (2009). Deregulation of microRNA involved in hematopoiesis and the immune response in HTLV-I adult T-cell leukemia. Blood *113*, 4914–4917.

Caretti, G., Di Padova, M., Micales, B., Lyons, G.E., and Sartorelli, V. (2004). The Polycomb Ezh2 methyltransferase regulates muscle gene expression and skeletal muscle differentiation. Genes Dev. *18*, 2627–2638.

Chen, Y., Takita, J., Choi, Y.L., Kato, M., Ohira, M., Sanada, M., Wang, L., Soda, M., Kikuchi, A., Igarashi, T., et al. (2008). Oncogenic mutations of ALK kinase in neuroblastoma. Nature *455*, 971–974.

Davis, B.N., Hilyard, A.C., Lagna, G., and Hata, A. (2008). SMAD proteins control DROSHA-mediated microRNA maturation. Nature *454*, 56–61.

Fiskus, W., Wang, Y., Sreekumar, A., Buckley, K.M., Shi, H., Jillella, A., Ustun, C., Rao, R., Fernandez, P., Chen, J., et al. (2009). Combined epigenetic therapy with the histone methyltransferase EZH2 inhibitor 3-deazaneplanocin A and the histone deacetylase inhibitor panobinostat against human AML cells. Blood *114*, 2733–2743.

Hayden, M.S., and Ghosh, S. (2008). Shared principles in NF-kappaB signaling. Cell *132*, 344–362.

Hironaka, N., Mochida, K., Mori, N., Maeda, M., Yamamoto, N., and Yamaoka, S. (2004). Tax-independent constitutive IkappaB kinase activation in adult T-cell leukemia cells. Neoplasia *6*, 266–278.

Horie, R., Watanabe, M., Ishida, T., Koiwa, T., Aizawa, S., Itoh, K., Higashihara, M., Kadin, M.E., and Watanabe, T. (2004). The NPM-ALK oncoprotein

abrogates CD30 signaling and constitutive NF-kappaB activation in anaplastic large cell lymphoma. Cancer Cell *5*, 353–364.

Iwanaga, M., Watanabe, T., Utsunomiya, A., Okayama, A., Uchimaru, K., Koh, K.R., Ogata, M., Kikuchi, H., Sagara, Y., Uozumi, K., et al; Joint Study on Predisposing Factors of ATL Development investigators. (2010). Human T-cell leukemia virus type I (HTLV-1) proviral load and disease progression in asymptomatic HTLV-1 carriers: a nationwide prospective study in Japan. Blood *116*, 1211–1219.

Kleer, C.G., Cao, Q., Varambally, S., Shen, R., Ota, I., Tomlins, S.A., Ghosh, D., Sewalt, R.G., Otte, A.P., Hayes, D.F., et al. (2003). EZH2 is a marker of aggressive breast cancer and promotes neoplastic transformation of breast epithelial cells. Proc. Natl. Acad. Sci. USA *100*, 11606–11611.

Liao, G., Zhang, M., Harhaj, E.W., and Sun, S.C. (2004). Regulation of the NF-kappaB-inducing kinase by tumor necrosis factor receptor-associated factor 3-induced degradation. J. Biol. Chem. *279*, 26243–26250.

Malinin, N.L., Boldin, M.P., Kovalenko, A.V., and Wallach, D. (1997). MAP3K-related kinase involved in NF-kappaB induction by TNF, CD95 and IL-1. Nature *385*, 540–544.

Min, J., Zaslavsky, A., Fedele, G., McLaughlin, S.K., Reczek, E.E., De Raedt, T., Guney, I., Strochlic, D.E., Macconaill, L.E., Beroukhim, R., et al. (2010). An oncogene-tumor suppressor cascade drives metastatic prostate cancer by coordinately activating Ras and nuclear factor-kappaB. Nat. Med. *16*, 286–294.

Prasad, S., Ravindran, J., and Aggarwal, B.B. (2010). NF-kappaB and cancer: how intimate is this relationship. Mol. Cell. Biochem. *336*, 25–37.

Ramakrishnan, P., Wang, W., and Wallach, D. (2004). Receptor-specific signaling for both the alternative and the canonical NF-kappaB activation pathways by NF-kappaB-inducing kinase. Immunity *21*, 477–489.

Saitoh, Y., Yamamoto, N., Dewan, M.Z., Sugimoto, H., Martinez Bruyn, V.J., Iwasaki, Y., Matsubara, K., Qi, X., Saitoh, T., Imoto, I., et al. (2008). Overexpressed NF-kappaB-inducing kinase contributes to the tumorigenesis of adult T-cell leukemia and Hodgkin Reed-Sternberg cells. Blood *111*, 5118–5129.

Sander, S., Bullinger, L., Klapproth, K., Fiedler, K., Kestler, H.A., Barth, T.F., Möller, P., Stilgenbauer, S., Pollack, J.R., and Wirth, T. (2008). MYC stimulates EZH2 expression by repression of its negative regulator miR-26a. Blood *112*, 4202–4212.

Schaefer, A., Jung, M., Mollenkopf, H.J., Wagner, I., Stephan, C., Jentzmik, F., Miller, K., Lein, M., Kristiansen, G., and Jung, K. (2010). Diagnostic and prognostic implications of microRNA profiling in prostate carcinoma. Int. J. Cancer *126*, 1166–1176.

Simon, J.A., and Kingston, R.E. (2009). Mechanisms of polycomb gene silencing: knowns and unknowns. Nat. Rev. Mol. Cell Biol. *10*, 697–708.

Sparmann, A., and van Lohuizen, M. (2006). Polycomb silencers control cell fate, development and cancer. Nat. Rev. Cancer *6*, 846–856.

Su, I.H., Basavaraj, A., Krutchinsky, A.N., Hobert, O., Ullrich, A., Chait, B.T., and Tarakhovsky, A. (2003). Ezh2 controls B cell development through histone H3 methylation and Igh rearrangement. Nat. Immunol. *4*, 124–131.

Su, I.H., Dobenecker, M.W., Dickinson, E., Oser, M., Basavaraj, A., Marqueron, R., Viale, A., Reinberg, D., Wülfing, C., and Tarakhovsky, A. (2005). Polycomb group protein ezh2 controls actin polymerization and cell signaling. Cell *121*, 425–436.

Suh, J., and Rabson, A.B. (2004). NF-kappaB activation in human prostate cancer: important mediator or epiphenomenon? J. Cell. Biochem. *91*, 100–117.

Thu, Y.M., and Richmond, A. (2010). NF-κB inducing kinase: a key regulator in the immune system and in cancer. Cytokine Growth Factor Rev. *21*, 213–226.

Trabucchi, M., Briata, P., Garcia-Mayoral, M., Haase, A.D., Filipowicz, W., Ramos, A., Gherzi, R., and Rosenfeld, M.G. (2009). The RNA-binding protein KSRP promotes the biogenesis of a subset of microRNAs. Nature *459*, 1010–1014.

Valastyan, S., Reinhardt, F., Benaich, N., Calogrias, D., Szász, A.M., Wang, Z.C., Brock, J.E., Richardson, A.L., and Weinberg, R.A. (2009). A pleiotropically acting microRNA, miR-31, inhibits breast cancer metastasis. Cell *137*, 1032–1046.

Varambally, S., Dhanasekaran, S.M., Zhou, M., Barrette, T.R., Kumar-Sinha, C., Sanda, M.G., Ghosh, D., Pienta, K.J., Sewalt, R.G., Otte, A.P., et al. (2002). The polycomb group protein EZH2 is involved in progression of prostate cancer. Nature *419*, 624–629.

Varambally, S., Cao, Q., Mani, R.S., Shankar, S., Wang, X., Ateeq, B., Laxman, B., Cao, X., Jing, X., Ramnarayanan, K., et al. (2008). Genomic loss of microRNA-101 leads to overexpression of histone methyltransferase EZH2 in cancer. Science *322*, 1695–1699.

Ventura, A., and Jacks, T. (2009). MicroRNAs and cancer: short RNAs go a long way. Cell *136*, 586–591.

Watanabe, M., Ohsugi, T., Shoda, M., Ishida, T., Aizawa, S., Maruyama-Nagai, M., Utsunomiya, A., Koga, S., Yamada, Y., Kamihira, S., et al. (2005). Dual targeting of transformed and untransformed HTLV-1-infected T cells by DHMEQ, a potent and selective inhibitor of NF-kappaB, as a strategy for chemoprevention and therapy of adult T-cell leukemia. Blood *106*, 2462–2471.

Yamagishi, M., Ishida, T., Miyake, A., Cooper, D.A., Kelleher, A.D., Suzuki, K., and Watanabe, T. (2009). Retroviral delivery of promoter-targeted shRNA induces long-term silencing of HIV-1 transcription. Microbes Infect. *11*, 500–508.

Yamaguchi, K., and Watanabe, T. (2002). Human T lymphotropic virus type-I and adult T-cell leukemia in Japan. Int. J. Hematol. *76* (*Suppl 2*), 240–245.

Yeung, M.L., Yasunaga, J., Bennasser, Y., Dusetti, N., Harris, D., Ahmad, N., Matsuoka, M., and Jeang, K.T. (2008). Roles for microRNAs, miR-93 and miR-130b, and tumor protein 53-induced nuclear protein 1 tumor suppressor in cell growth dysregulation by human T-cell lymphotrophic virus 1. Cancer Res. *68*, 8976–8985.

Zarnegar, B.J., Wang, Y., Mahoney, D.J., Dempsey, P.W., Cheung, H.H., He, J., Shiba, T., Yang, X., Yeh, W.C., Mak, T.W., et al. (2008a). Noncanonical NF-kappaB activation requires coordinated assembly of a regulatory complex of the adaptors cIAP1, cIAP2, TRAF2 and TRAF3 and the kinase NIK. Nat. Immunol. *9*, 1371–1378.

Zarnegar, B.J., Yamazaki, S., He, J.Q., and Cheng, G. (2008b). Control of canonical NF-kappaB activation through the NIK-IKK complex pathway. Proc. Natl. Acad. Sci. USA *105*, 3503–3508.

成人T細胞白血病から明らかになった新たなクロストーク経路の異常とがん

山岸 誠・渡邉俊樹

（東京大学大学院新領域創成科学研究科 メディカルゲノム専攻病態医療科学分野）

email：山岸 誠，渡邉俊樹

Polycomb-mediated loss of miR-31 activates NIK-dependent NF-κB pathway in adult T cell leukemia and other cancers.
Makoto Yamagishi, Kazumi Nakano, Ariko Miyake, Tadanori Yamochi, Yayoi Kagami, Akihisa Tsutsumi, Yuka Matsuda, Aiko Sato-Otsubo, Satsuki Muto, Atae Utsunomiya, Kazunari Yamaguchi, Kaoru Uchimaru, Seishi Ogawa, Toshiki Watanabe
Cancer Cell, 21, 121-135 (2012) http://www.ncbi.nlm.nih.gov/pubmed/22264793

要 約

成人T細胞白血病は日本人に100万人以上，世界では推定2000万人の感染者がいるHTLV-1によりひき起こされる重篤な白血病で，有効な治療法は確立していない．筆者らは，HTLV-1感染者コホート共同研究班の全面的な協力を得て，世界ではじめて成人T細胞白血病患者の細胞のゲノム，mRNA，マイクロRNAの大規模な統合解析を完了した．その結果，成人T細胞白血病の悪性化をひき起こす原因として，マイクロRNAのひとつmiR-31がすべての成人T細胞白血病患者において著しく減少していることを明らかにした．miR-31の減少はその標的遺伝子の産物であるNIKの過剰な発現とそれにともなうNF-κBシグナルの恒常的な活性化を誘発すること，miR-31を再導入すると細胞死が誘導されることが示された．ゲノムの欠損およびPolycombファミリーに依存的なエピジェネティックな異常がmiR-31の発現低下の原因であり，また，成人T細胞白血病だけでなく乳がん細胞やB細胞における免疫応答反応でも同じ機構が保存されていることがわかった．したがって，Polycombファミリー，miR-31，NIKのバランスが細胞の運命に重要であることが示された．Polycombファミリーは細胞の恒常性や分化などの多彩な機能に必須であると同時に，その異常は多くのがん細胞における重要な分子標的となっている．マイクロRNAを介したPolycombファミリーとNF-κBとのクロストークは新たな概念であり，この研究の成果より，エピジェネティックな異常がNF-κBシグナルの恒常的な活性化を介しアポトーシスに対する抵抗性の獲得に寄与することが明らかになった．

はじめに

成人T細胞白血病（adult T cell leukemia/lymphoma：ATL）はHTLV-1（human T cell leukemia virus type 1，ヒトT細胞白血病ウイルスI型）の感染によりひき起こされる重篤なT細胞性の白血病である．50〜60年という長い潜伏期間のあいだHTLV-1に感染した末梢血のT細胞には複数の遺伝子異常が蓄積しがん化がひき起こされる（図1）．現在，世界には2000万人以上の感染者がいるとされるが，わが国ではとくに多く，約120万人の感染者が存在し毎年1000人をこえる感染者がきわめて予後の不良な成人T細胞白血病を発症する．白血病やウイルスが発見された当時からこの分野における日本人研究者の貢献度は多大であるが，ウイルスによる細胞の不死化や腫瘍化，治療への抵抗性などの分子機構にはいまだに不明な点が多く残されており有効な治療法は存在しない．ウイルスの根絶と白血病の予防，新規の治療法の開発をめざした分子レベルでの病態の解明が必須である[1)]．

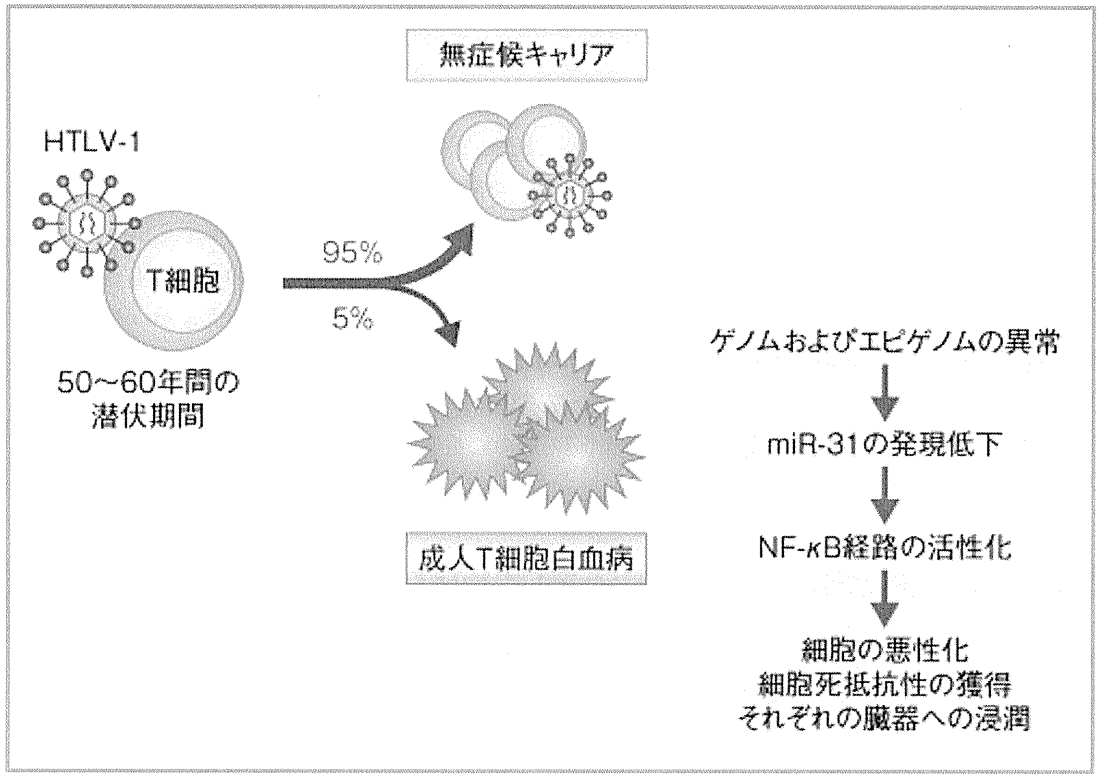

図1　HTLV-1の感染と成人T細胞白血病のモデル
成人T細胞白血病はHTLV-1感染者（キャリア）の約5%に発症する．成人T細胞白血病細胞はウイルス遺伝子の発現が低く，さまざまな遺伝子異常の蓄積によりシグナル伝達系の撹乱が起こっている．miR-31は成人T細胞白血病の全例において低下しており，腫瘍細胞の悪性化に寄与する．
[Download] http://first.lifesciencedb.jp/wordpress/wp-content/uploads/2012/02/Watanabe-Cancer-Cell-12.1.17-Fig.1.jpg

成人T細胞白血病細胞およびHTLV-1感染細胞の生物学的な特徴として恒常的なNF-κBシグナルの活性化があり，これにより細胞の異常な増殖および生存が確保されている[2]．HTLV-1感染細胞ではウイルスの遺伝子産物であるTaxがNF-κBの定型的（canonical）経路および非定型的（noncanonical）経路を劇的に活性化するが，通常はTaxの発現が認められない成人T細胞白血病細胞におけるNF-κBシグナルの活性化の機構には不明な点が多かった．そののち，遺伝子発現の解析によりNIK（NF-κB-inducing kinase）をコードするmRNAの過剰な発現が恒常的なNF-κBシグナルの活性化に寄与していることが明らかになっているが[3]，NIKの異常発現の機構は明らかになっていなかった．NF-κBシグナルの異常な活性化とそれにともなう腫瘍細胞の生存能の獲得および悪性化は，成人T細胞白血病だけでなく多くの固形がんや悪性リンパ腫，白血病において共通してみられるがん細胞の特徴のひとつである．そのなかでも，NIKの高発現による異常な活性化は重要な位置をしめているが，正常を逸脱するその機構は不明でありがん研究の全体における課題であった．

筆者らは，成人T細胞白血病患者のマイクロRNAの解析，mRNAの発現解析，および，ゲノム異常の解析を統合してその分子病態の全貌にアプローチした．その結果として明らかになった成人T細胞白血病における分子異常はその臨床的な特徴をよく反映しており，分子マーカーや治療標的としてさまざまな情報を提示した．さらに，明らかにされた新たな分子機構はがん研究の全体に新たな概念を提唱した．

1．成人T細胞白血病の臨床検体を用いた大規模な統合解析からみる分子病態

これまでの成人T細胞白血病の研究の多くは細胞株か少数の患者に由来する細胞から得られた情報を基盤としたものであり，実際の成人T細胞白血病細胞を分子レベルで正確に理解することが成人T細胞白血病の研究において重要な課題であった．いまだ有効な治療法のない成人T細胞白血病に対し根本的な情報を得る

ため，筆者らはまず，全国的なHTLV-1疫学調査および検体バンク組織であるHTLV-1感染者コホート共同研究班（JSPFAD，URL：http://htlv1.org/）の全面的な協力を得て，成人T細胞白血病の臨床検体を用いたマイクロRNAおよびmRNAの大規模な解析に着手した．米国Agilent Technologies社のマイクロRNAマイクロアレイを用い，成人T細胞白血病細胞40例，正常なCD4陽性T細胞22例について解析を行った結果，非常に厳しい検定をクリアした61個のマイクロRNAにおける発現異常を同定した．ほかのがん細胞における報告と同様に，成人T細胞白血病細胞では発現の異常を示すマイクロRNAのほとんどは発現の低下を示した．成人T細胞白血病細胞におけるマイクロRNAの発現パターンはユニークで，マイクロRNAの発現をもって正常なT細胞と区別できることもわかった．この61個のマイクロRNAのなかでもっとも差の大きかったmiR-31は，正常なT細胞では比較的発現量が高く，一方で，成人T細胞白血病細胞では非常に発現が低いもしくは検出限界以下にまで発現が低下していた．miR-31は乳がん細胞の転移能をはじめさまざまな細胞機能にかかわる重要なマイクロRNAで4)，その発現の低下が細胞の運命に重要な意味を包含するものと考えられた．

2. miR-31の発現低下とその生物学的な意義

マイクロRNAのおもな生物学的な機能は標的遺伝子の3'側非翻訳領域に結合することによりその発現を負に制御することである．外来の合成siRNAとは異なり，マイクロRNAによる配列の認識はゆらぎが特徴的であり，ひとつのマイクロRNAが複数個の遺伝子を制御することができる．細胞の運命に重大な影響をあたえるような標的遺伝子の探索には，物理的な抑制効果と同時に標的遺伝子の側の機能や挙動も重要な指標となり，したがって，多角的な実験的検証が必須になる．筆者らは，成人T細胞白血病の全例で発現が低下していたmiR-31のT細胞における生物学的な意義を明らかにするため，以下の検討を行った．1）miR-31の標的遺伝子を4つのアルゴリズムにより予測，2）成人T細胞白血病細胞のmRNAの大規模な解析データとのすりあわせによる検証，3）変異を導入したレポーターアッセイ，4）miR-31の増減に対する候補となる標的遺伝子の定量，5）miR-31と標的遺伝子との関係の保存性の確認．以上により，NIKをコードする遺伝子がmiR-31の新規の標的遺伝子であることが明らかになった．NIKはNF-κBの非定型的経路の活性化に必須のリン酸化酵素であり，その発現量がNF-κBシグナルの恒常的な活性化に直接的に寄与することが複数のがんにおいて報告されている．成人T細胞白血病ではNIKをコードするmRNAの量が増加していることがわかっていたが3)，過剰な発現の原因は明らかにされていなかった．成人T細胞白血病患者に由来する細胞から樹立された細胞株にmiR-31を過剰に発現させるとNIKのmRNA量およびタンパク質量が低下し，NF-κBシグナルが低下することがわかった．これらの細胞では増殖能の低下，抗アポトーシス遺伝子の発現の低下，アポトーシス感受性の向上がみられた．さらに，miR-31を発現誘導するレンチウイルスベクターは成人T細胞白血病患者から直接取り出した腫瘍細胞のアポトーシスを誘導することがわかった．以上より，miR-31の発現の低下は成人T細胞白血病細胞の生存にとって重要であり，その分子機構はNIKの過剰な発現の誘導であることが示された．NF-κBシグナルは非常に複雑な制御機構を備えているが，miR-31が新たなNF-κBシグナルの抑制因子として同定された．

3. ゲノムおよびエピゲノムの異常とmiR-31の発現制御

細胞内での成熟したマイクロRNAのダイナミズムは，転写制御および転写後の成熟過程の制御により規定されている．成人T細胞白血病の全例で発現の低下のみられたmiR-31は転移性乳がんや前立腺がんなどでも発現が低下しており，がん細胞における一般性と重要性が示唆されたが，細胞内においてmiR-31の量がどのように制御されているかについては不明であった．*miR-31*遺伝子は多くのがん細胞でゲノムの欠失が頻発する9p21.3の*CDKN2A/B*領域に隣接しており，成人T細胞白血病においてもゲノムの不安定性が予測された．成人T細胞白血病168症例での大規模なDNAコピー数の解析の結果，12.5%の症例で*miR-31*遺伝子のホモもしくはヘテロの欠損のあることがわかった．一方で，同時に行ったマイクロRNAの発現解析では，ゲノムの欠損のない症例でも正常なT細胞に比べmiR-31の量が大きく減少していることがわかった．そこで，発現解析データとアルゴリズムから*miR-31*遺伝子の転写構造を予測したところ，miR-31

は*LOC554202*遺伝子のイントロン領域にコードされ，独立した転写が起こっていることがわかった．また興味深いことに，YY1という転写因子の認識配列が*miR-31*遺伝子の転写開始点の上流に蓄積していた．このYY1はPolycombファミリーに属するDNA結合タンパク質で，ヒストンH3の27番目のリジン残基のメチル化酵素であるEZH2をはじめとするPRC2（Polycomb repressive complex 2）のリクルーターとしての機能が注目されている[5]．そこで，YY1のノックダウン実験を行ったところ，*miR-31*遺伝子領域へのYY1の蓄積が減少し，それに付随してEZH2のリクルートが減少することがわかった．

では，成人T細胞白血病細胞をはじめとする高悪性度の腫瘍において，なぜmiR-31の発現が激減するのか？　成人T細胞白血病におけるmRNAの発現解析の結果，ヒストンH3の27番目のリジン残基のトリメチル化を誘導するPolycombファミリーに属するEZH2およびSUZ12をコードする遺伝子の発現が正常なT細胞に比べ高いことがわかった．成人T細胞白血病細胞株においてこれらPolycombファミリーをノックダウンすると，*miR-31*遺伝子領域へのPRC2のリクルートが減少し，その結果，ヒストンH3の27番目のリジン残基および9番目のリジン残基のメチル化レベルが低下した．さらに，ヒストンの脱アセチル化を介して転写抑制にはたらくHDAC1の結合量も減少し，その結果，miR-31の発現が回復することがわかった．以上の実験データから，Polycombファミリーの発現異常がmiR-31の発現低下を誘導するという新たな分子機構が明らかになった．この事実は，成人T細胞白血病患者に由来する腫瘍細胞をクロマチン免疫沈降アッセイにより直接的に調べた結果，*miR-31*遺伝子領域に異常な抑制的メチル化をもつヒストンが検出され，また，EZH2のノックダウンが直接に細胞死を誘導したこと，さらに，同様の分子機構が好転移性乳がん細胞やB細胞株においても保存されていたことからもサポートされた．

以上より，細胞内における成熟miR-31の発現量は，ゲノムの安定性と，YY1とPRC2によるエピジェネティックな制御の2つの側面により規定されていることが示された．

4．Polycombファミリーによる miR-31制御を介したNF-κB経路への影響

miR-31はNIKのほかRhoA，Radixin，インテグリンα5，FoxP3，FIH，E2F2などさまざまなタンパク質をコードする遺伝子を負に制御し細胞の運命に強く影響する．一方で，miR-31を制御するPolycombファミリーは多くの悪性リンパ腫，白血病，固形がんの増殖，生存，転移能に重要であるが，どの標的遺伝子が細胞の表現型に直接に影響するかについては不明な点が多かった．そこで，この研究で明らかになったmiR-31によるNIKを介したNF-κB経路の制御とPolycombファミリーによるmiR-31の発現制御とをあわせ，Polycombファミリーによるエピジェネティックな制御がNIKに依存的なNF-κB経路の制御にかかわるという仮説をたてた．これまで，PolycombファミリーとNF-κB経路との関係は不明であった．

成人T細胞白血病細胞株においてEZH2もしくはSUZ12をノックダウンすると，さきに述べたようにmiR-31の発現が誘導され，このとき，NIKの量が減少することにより下流へのシグナルが停止しNF-κBシグナルが低下した．さらに，これらの細胞では細胞の増殖および細胞死への抵抗性が低下した．Polycombファミリー，miR-31，NIKはそれぞれの経路の上流に位置し，細胞に対するアウトプットはさまざまに拡散すると考えられるが，以下の実験事実によりこの分子機構は非常に重要であると考えられた．1）Polycombファミリーのノックダウンにより低下したNF-κBシグナルはmiR-31の阻害剤を共存させることにより回復することから，PolycombファミリーによるNF-κBの制御にはmiR-31の仲介が重要である，2）Polycombファミリーのノックダウンにより誘導される成人T細胞白血病細胞の強制的なアポトーシスは3'側非翻訳領域を削除したNIKによりレスキューされる，つまり，Polycombファミリーにより獲得された異常な生存能の一部はNIKにより具現化されている．3）miR-31の過剰な発現やPolycombファミリーのノックダウンはB細胞におけるBAFFやCD40LからのNF-κBの非定型的経路の活性化を阻害することから，がん細胞のシグナルだけでなく正常細胞のシグナルの制御にも重要である．4）miR-31の発現およびPolycombファミリーのノックダウンにより成人T細胞白血病細胞のMDC（CCR4リガンド）に対する走化性が低下し，NIK以外のmiR-31の標的遺伝子による表現型はPolycombファミリーによっても影響をうける．

5. 新規の治療法の開発へ

Polycombファミリーの過剰な発現，miR-31の発現の低下，NIK量の増加とNF-κBシグナルの恒常的な活性化は，いずれも成人T細胞白血病の臨床検体から明らかになった．この研究の総括として，この腫瘍細胞の分子レベルでの特徴が細胞の生存にどのように影響するかを検討した．miR-31の強制発現，また，EZH2もしくはNIKのノックダウンを行うレンチウイルスベクターを作製し，患者に由来する腫瘍細胞に直接に導入することにより*ex vivo*での評価を行った．その結果，ある程度の個人差をもっていずれのレンチウイルスも複数の成人T細胞白血病の症例で強烈なアポトーシスを誘導することがわかった．同様の処理は正常の末梢血の単核球もしくはT細胞に対しては効果が微弱であり，それぞれの因子の存在量のバランスの異常が成人T細胞白血病細胞の生存に重要であることが示された．これらの結果は，miR-31が成人T細胞白血病細胞に特異的な細胞障害性をもつことを示しており，この細胞に特異的な導入法を開発することにより成人T細胞白血病の新規の治療法につながる可能性をもつと考えられた．

おわりに

この研究は，成人T細胞白血病における新たな分子標的とNF-κBシグナルの活性化の機序を明らかにするとともに，Polycombファミリーによるエピジェネティックな制御，マイクロRNAによる細胞運命の決定，NF-κB経路による免疫細胞および腫瘍細胞の分子基盤，という3つのコンテクストに新たな生物学的なリンクを見い出した（図2）．また，この研究で得られた知見は以下の点で重要であった．

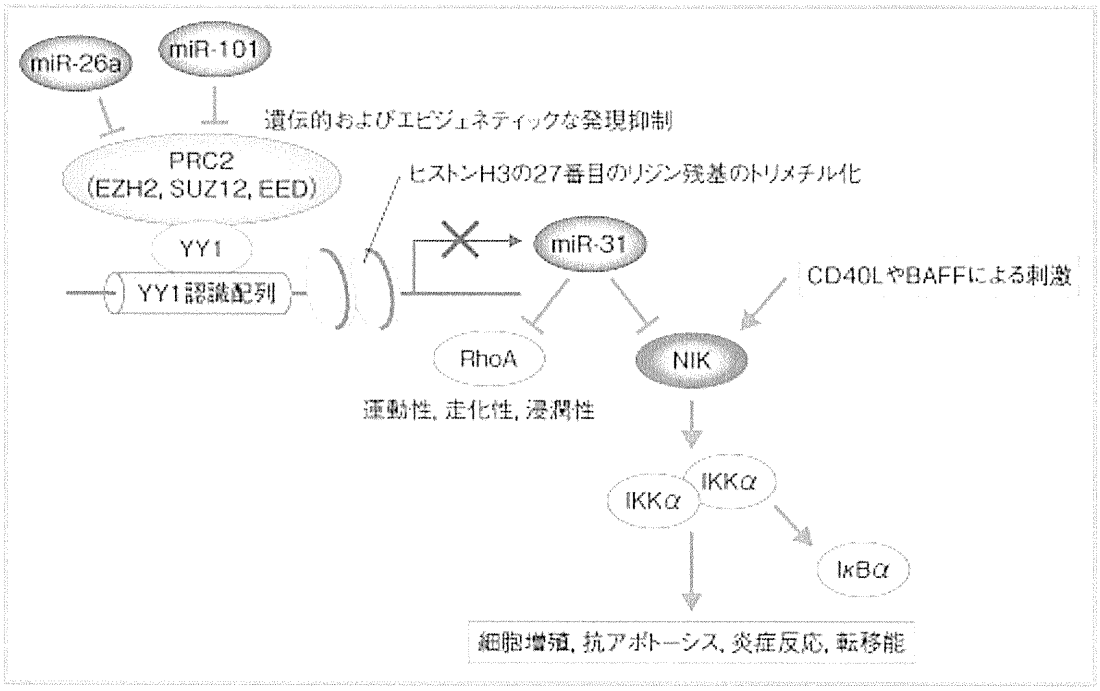

図2　Polycombファミリーに依存的なmiR-31の発現低下はNIKなどの標的遺伝子を介して細胞の表現型に影響する
これらの因子のあいだの関係はさまざまな細胞で保存されており，それぞれの因子の存在量のバランスにより均衡が保たれている．バランスをくずした細胞は悪性化をたどるものと考えられる．
[Download] http://first.lifesciencedb.jp/wordpress/wp-content/uploads/2012/02/Watanabe-Cancer-Cell-12.1.17-Fig.2.jpg

1つ目は，NIKの新たな制御機構を明らかにしたことである．NIKは成人T細胞白血病以外にも，多発性骨髄腫，悪性リンパ腫，乳がんなどにおけるNF-κBシグナルの異常な活性化の原因タンパク質である．また，NIKは免疫担当細胞をはじめとする種々の細胞の正常機能に必須であり，NIKをめぐる基礎研究は注目をあつめている．NF-κB経路の複雑な制御系にmiR-31が組み込まれていること，さらに，Polycombファミリーに依存的なエピジェネティックな制御がマイクロRNAを介してNF-κBシグナルの制御に寄与するとい

う発見は，今後のシグナル伝達の研究に対し大きく貢献するものと考えられる．

2つ目は，Polycombファミリーはマイクロ RNAの発現を制御することにより，より多くの遺伝子の発現につき転写および翻訳の段階において影響力をもつ可能性のあることである．また，Polycombファミリー自体も複数のマイクロRNAにより制御されていることがわかっている．現に，成人T細胞白血病においてはEZH2を抑制するマイクロRNAが減少していた．

3つ目は，Polycombファミリーによる標的配列の認識機構の一端を明らかにしたことである．PRC2による標的配列の認識はYY1だけでは説明できないことは複数の研究により示されているが，miR-31のようにYY1結合配列の蓄積という特殊なケースが細胞に対する影響力の大きい可能性がある．

4つ目は，シグナルのクロストークと細胞の正常機能についてである．この研究で得られた知見はそれぞれの鍵となる因子の異常な挙動を指標として明らかになったが，それぞれの因子は元来，細胞の恒常性や正常機能に重要であると考えられる．がん研究から得られた知見がより基礎的および臨床的な理解に貢献することを期待したい．

最後に，miR-31の成人T細胞白血病に対する分子標的薬としての応用の可能性が示されたといえる．今後の研究により実用化が可能となれば，成人T細胞白血病のみならず同様の分子病態を示すがんの新たな治療法の開発の先例となる可能性がある．

文献

1. Iwanaga, M., Watanabe, T., Utsunomiya, A. et al.: **Human T-cell leukemia virus type I (HTLV-1) proviral load and disease progression in asymptomatic HTLV-1 carriers: a nationwide prospective study in Japan.** Blood, 116, 1211-1219 (2010)[PubMed http://www.ncbi.nlm.nih.gov/pubmed/20448111]
2. Watanabe, M., Ohsugi, T., Shoda, M. et al.: **Dual targeting of transformed and untransformed HTLV-1-infected T cells by DHMEQ, a potent and selective inhibitor of NF-κB, as a strategy for chemoprevention and therapy of adult T-cell leukemia.** Blood, 106, 2462-2471 (2005)[PubMed http://www.ncbi.nlm.nih.gov/pubmed/15956280]
3. Saitoh, Y., Yamamoto, N., Dewan, M. Z. et al.: **Overexpressed NF-κB-inducing kinase contributes to the tumorigenesis of adult T-cell leukemia and Hodgkin Reed-Sternberg cells.** Blood, 111, 5118-5129 (2008) [PubMed http://www.ncbi.nlm.nih.gov/pubmed/18305221]
4. Valastyan, S., Reinhardt, F., Benaich, N. et al.: **A pleiotropically acting microRNA, miR-31, inhibits breast cancer metastasis.** Cell, 137, 1032-1046 (2009)[PubMed http://www.ncbi.nlm.nih.gov/pubmed/19524507]
5. Simon, J. A. & Kingston, R. E.: **Mechanisms of polycomb gene silencing: knowns and unknowns.** Nat. Rev. Mol. Cell Biol., 10, 697-708 (2009)[PubMed http://www.ncbi.nlm.nih.gov/pubmed/19738629]

著者プロフィール

山岸 誠（Makoto Yamagishi）

略歴：2009年 東京大学大学院新領域創成科学研究科 修了，同年 エイズ予防財団 リサーチレジデントを経て，2011年より東京大学大学院新領域創成科学研究科 特任研究員．

研究テーマ：白血病およびリンパ腫における分子病態，とくに，エピジェネティクス，マイクロRNA，シグナル伝達．HIVの潜伏化の分子機構．

関心事：腫瘍細胞および正常細胞におけるエピジェネティクス，マイクロRNA，シグナル伝達系のクロストーク．基礎研究から発信する情報を臨床へフィードバックすることをめざしたい．

渡邉 俊樹（Toshiki Watanabe）

東京大学大学院新領域創成科学研究科 教授

研究室URL：http://www.ims.u-tokyo.ac.jp/ltcb-mgs/

血液内科，62(4)：455-462，2011

特集　分子病態からみた血液疾患診療の進歩

ATLの分子病態と治療の新展開*

渡邉俊樹**

Key Words：micro RNA, signal transduction, molecular targeted therapy, antibody therapy

はじめに

2007年の献血者の抗体陽性率に基づく推定によると，わが国のHTLV-1感染者数は人口の約1％に近い108万人にのぼる[1]．また，厚生労働省の人口動態統計によると毎年1,000人以上が成人T細胞白血病(ATL)で死亡しており，同省研究班の全国調査によると，ATLの患者数は1,146例/年と推計された[1]．これらの事実は，ATLは疾患概念の確立および原因ウイルスHTLV-1の同定から30年を過ぎても，いまだに，わが国において，深刻ながんの一つであることを示している．ウイルス感染細胞のがん化の分子機構は「多段階発がん機構」によることは示されているが，それに関与する具体的な遺伝子の実態に関してはいまだに不明である(図1)．発症を予防する「発症予防法」の研究も進んでいない[1]．

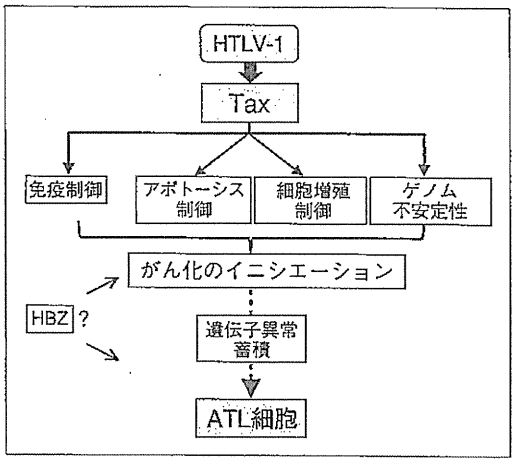

図1　HTLV-1の細胞腫瘍化機構
HTLV-1感染で発症するATLは多段階発がん機構によって発症する．ウイルスのがん遺伝子Taxは強力かつ多彩な機能を持ち，免疫制御，アポトーシス制御，細胞増殖，ゲノム不安定性のすべてに関与するが，ATL細胞ではウイルスゲノムが欠損・変異したり，エピジェネティックに抑制されており，発現は認められない．したがって，イニシエーションに関与すると考えられている．HBZの作用に関する分子機序は明らかではない．

ATL研究は，他のがんと同様に，その発症機構解明を通じた発症予防法・新規治療法開発による患者の救済を究極の目標とする．しかし，ATL研究の独自性は，そのアプローチに2つの道があることである．まず，HTLV-1感染細胞がウイルスの作用によって，最終的にはがん化するという事実から，ウイルスの遺伝子産物の作用という視点からの病原性発現機構解析である．この視点からは他の関連疾患の発症機構も視野に入ってくるであろう．もう一方の視点は，他のがん研究と共通するものであり，腫瘍細胞＝ATL細胞の解析を通じたアプローチである．ATL細胞の種々の分子細胞生物学的な表現型は，遺伝子

* Recent advances in molecular pathology and therapy of ATL.

** Toshiki WATANABE, M.D., Ph.D.: 東京大学大学院新領域創成科学研究科メディカルゲノム専攻〔〒108-8639 東京都港区白金台4-6-1〕; Department of Medical Genome Sciences, Graduate School of Frontier Sciences, The University of Tokyo, Tokyo 108-8639, JAPAN

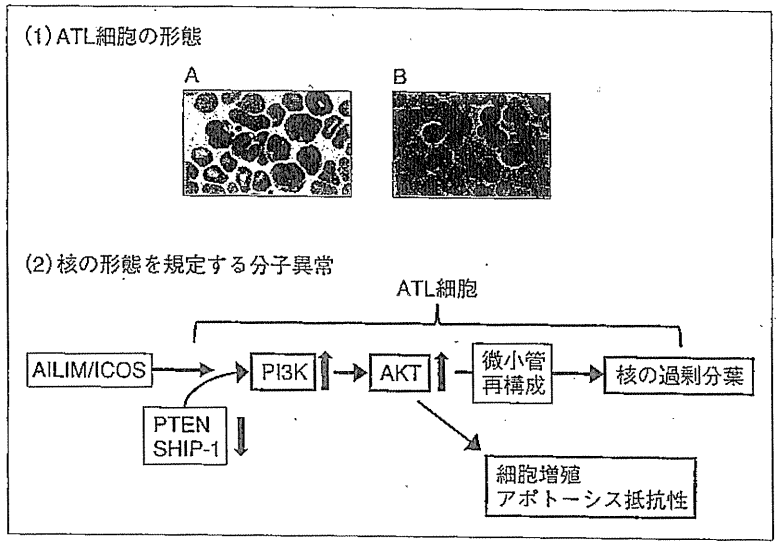

図2　末梢血のATL細胞と「花細胞」の分子基盤
(1)ATL患者末梢血像(今村病院分院 宇都宮與博士提供)．A：急性型ATLの末梢血．ATL細胞は核の変形が著明である．B：慢性型ATLの末梢血．やや小型であるが核の分葉やくびれを認める．(2)PTENやSHIP-1の抑制によるPI3-kinase, AKTの恒常的活性化が微小管の再構成を介して特徴的な分葉核を形成している．

異常の集積の結果を反映している．したがって，ATL細胞の分子病態を理解することは，単に診断のみならず腫瘍化機構の理解，さらには発症予防や治療を考える上で重要かつ必須の作業である[2]．

本稿では，ウイルス感染後約50年の臨床的潜伏期に腫瘍化イベントを蓄積した結果であるATL細胞の分子病態解析の現状を整理するとともに，ATL治療研究のまとめと，新規治療法の試みについて紹介することにする．

ATL細胞の分子病態

ATL細胞の細胞学的あるいは分子生物学的な特徴についてはこれまでに多数の報告が蓄積されている．以下にその概略をまとめる．

1．ATL細胞の細胞生物学的特徴

(1)花細胞の分子基盤

末梢血におけるATL細胞は典型的には「花細胞=flower cell」と呼ばれ，過分葉してクロマチンの濃縮した核を持ち，普通明確な核小体を示さない(図2)．この特有の核の形態は，ATL細胞のAILIM/ICOSシグナルによるPI3-kinaseの活性化によることが報告されている[3]．

(2)ATL細胞の膜抗原の発現

典型的には$CD3^{dull}CD4^{+}CD8^{-}CD25^{+}HLA\text{-}DR^{+}$とされるが，CD25やHLA-DRの発現は全例に認められるわけではない．$CD4^{+}CD8^{+}$の例は約7％であり，$CD4^{-}CD8^{-}$も7％，$CD4^{-}CD8^{+}$の症例も4％の割合であると報告されている[4]．最近の報告では，急性型ATL患者の末梢血リンパ球をmulti-color FACSで検討し，腫瘍細胞が$CD3^{dim}CD7^{low}$の$CD4^{+}$Tリンパ球分画に対応することが確認された[5]．末梢血中の腫瘍細胞集団を同定しその細胞生物学的表現型を解析する上で有用な情報であると考えられる．

(3)ATL細胞はTregか？

ATL細胞で，FoxP3およびCTLA-4の発現があることから，一部には「ATLは制御性T細胞(Treg)が腫瘍化したものである」との考えがある．しかし，このようなとらえ方は早計であると判断せざるを得ない．多くの報告から，FoxP3およびCTLA-4の発現が半数あるいはそれ以下の例に限られること，in vitroでの$CD4^{+}$あるいは$CD8^{+}$Tリンパ球の増殖抑制能を持つのはさらにその一部であることが確認されている[6)-9)]．したがって，ATL細胞におけるFoxP3等の発現は，制御性T細